Supplementary materials

Supplementary material A: Consistency of the results obtained for datasets built with a maximum error rate tolerance of 0.5 with datasets built with a maximum error rate tolerance of 0.1

1. Relative abundance

The best model obtained with the dredge (i.e., the one with the lowest AICc – second order bias correction for Akaike information criterion) was the following one:

Relative abundance metric ~ Conifer_forest + Deciduous_forest + Julian_day + Moonlight + Small_woody_features + Habitat_diversity + ALAN + Cloud_cover + Difference_precipitations + Difference_temperature + Temperature + Latitude + Recorder_type + (1 | site / participation) Eq. (A.1)

In Table A.1, we can see that the results were highly consistent whether the maximum error rate tolerance (MERT) chosen was 0.5 or 0.1. The variables which were significant in the best model with the 0.5 MERT remained significant with the 0.1 MERT, estimates that were negative remained negative and estimates that were positive remained positive.

Table A.1: Best model estimates and p-values (Anova II) for the "relative abundance" dataset with a MERT of 0.5 and 0.1. Latitude and recorder type are not represented as they were fixed terms in the dredge. All quantitative fixed effects were scaled.

MERT	**0.5**		**0.1**	
	Estimate	**p-value**	**Estimate**	**p-value**
Conifer_forest	0.3523	9.776e-06 ***	0.5109	1.048e-07 ***
Deciduous_forest	0.2659	0.0001009 ***	0.2725	0.0007871 ***
Julian_day	0.3330	2.792e-08 ***	0.4641	7.438e-10 ***
Moonlight	-0.1641	0.0019158 **	-0.2748	1.486e-05 ***
Small_woody_features	0.1945	0.0050122 **	0.1867	0.0261389 *
Habitat_diversity	0.1938	0.0109567 *	0.3240	0.0004355 ***
ALAN	-0.4374	1.481e-06 ***	-0.6077	1.476e-07 ***
Cloud_cover	0.0719	0.1155775	0.0004	0.9943969
Difference_precipitations	-0.1643	0.0006891 ***	-0.2604	1.457e-05 ***
Difference_temperature	0.3077	5.430e-07 ***	0.3816	8.046e-08 ***
Temperature	0.2659	8.719e-05 ***	0.2289	0.0045416 **

2. Timing of activity

The best model obtained with the dredge (i.e., the one with the lowest AICc) was the following one:

$$\textit{Timing of activity metric} \sim \textit{Julian\_day} + \textit{Julian\_day}^2 + \textit{Moonlight} + \textit{ALAN} + \textit{Cloud\_cover} + \textit{Difference\_precipitations} + \textit{Difference\_temperature} + \textit{Wind\_speed} + \textit{Latitude} + \textit{autocov} + \textit{Moonlight : ALAN} + \textit{ALAN : Cloud\_cover} + (1 \mid \textit{site}) \quad \text{Eq. (A.2)}$$

In Table A.2, we can see that, apart from ALAN, results were highly consistent whether the MERT chosen was 0.5 or 0.1. The variables which were significant in the best model with the 0.5 MERT remained significant with the 0.1 MERT, estimates that were negative remained negative and estimates that were positive remained positive.

Table A.2: Best model estimates and p-values (Anova II) for the "timing of activity" dataset with MERT of 0.5 and 0.1. Latitude and autocov are not represented as they were fixed terms in the dredge. All quantitative fixed effects were scaled.

MERT	**0.5**		**0.9**	
	Estimate	**p-value**	**Estimate**	**p-value**
Julian_day	-86.20	0.5302259	328.18	0.0884699 .
Julian_day²	354.78	0.0005707 ***	489.54	0.0008973 ***
Moonlight	291.01	0.0087162 **	334.29	5.815e-06 ***
ALAN	734.67	0.0001537 ***	-321.00	0.2231442
Cloud_cover	- 481.49	1.411e-12 ***	-410.73	1.852e-09 ***
Difference_precipitations	-164.92	0.0243367 *	-299.76	0.0027053 **
Difference_temperature	378.70	5.571e-08 ***	304.23	0.0006953 ***
Windspeed	-292.33	2.300e-05 ***	-306.21	0.0001368 ***
Moonlight : ALAN	-264.33	0.0016276 **	-1233.08	3.010e-08 ***
ALAN : Cloud_cover	178.24	0.0174029 *	457.85	0.0001788 ***

Despite being highly significant with a 0.5 MERT, ALAN became not significant with a 0.1 MERT. By choosing a low MERT, we only kept 11,513 *E. serotinus* passes instead of 22,998 with a 0.5 MERT (i.e., -50% of passes) (Table A.3). The calculation of the timing of activity (i.e., the time of the median *E. serotinus* pass during the first 4 h 30 min of the night) may hence have been be less precise, and, as we only considered nights with at least 10 *E. serotinus* passes, it also led us to take into account less nights and sites. We may therefore have lost too much statistical power to detect any effect of ALAN.

To check it, we performed a power analysis to assess, with a 0.5 MERT, the minimum number of passes needed to detect an effect of ALAN on the timing of activity. To do so, we generated subsets of our dataset with a 0.5 MERT based on a selection of 1000 to 22,750 *E. serotinus* passes. For each number of passes, we generated 200 subsets, we removed nights

with less than 10 passes and recalculated the time of the median pass for each night. Then, on each subset, we ran our best model to extract ALAN estimate and p-value (Anova II). Finally, we computed the percentage of the 200 models, for each number of passes, for which ALAN estimate was positive with a significant p-value. When more than 80% of ALAN estimates were positive with a significant p-value, we concluded that the statistical power was strong enough to detect an ALAN effect on the timing of activity. We draw this percentage according to the number of *E. serotinus* passes in the dataset (Fig. A.1). We concluded that a minimum of roughly 13,500 passes should be included in the analyses to detect an effect of ALAN on the timing of activity, thus explaining why it was not detected with a 0.1 MERT which strongly restricted the number of *E. serotinus* passes to analyse.

Table A.3: Number of sites, nights and sounds kept for a 0.5 and a 0.1 MERT for the "relative abundance" and the "timing of activity" datasets.

	MERT	Number of passes all night	Number of passes first half of night
Relative abundance	**0.5**	21,452	/
	0.1	10,117	/
Timing of activity	**0.5**	22,998	19,489
	0.1	11,513	9,901

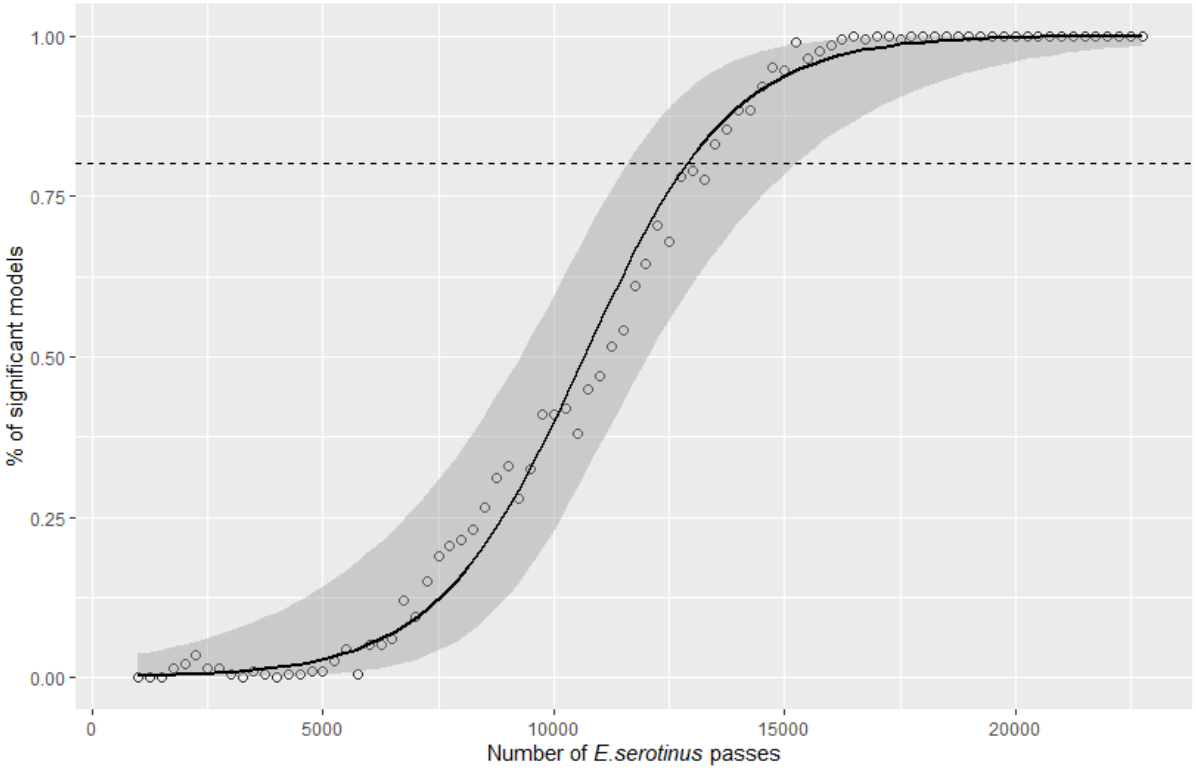

Fig. A.1: Power analysis results: for each number of *E. serotinus* passes (from 1000 to 22,750), percentage of subsets that resulted in a positive and significant estimate for ALAN. The dotted line represents the minimum 0.8 threshold below which the statistical power become insufficient. The solid curve represents the result of a binomial regression on the percentage of subsets that resulted in a positive and significant estimate for ALAN according to the number of *E. serotinus* passes.

Supplementary material B: Threshold on the number of *E. serotinus* passes for the "timing of activity" analyses

We postulated that no analysis of the timing of activity would be robust enough if there were not enough *E. serotinus* passes during the studied nights. Hence, we chose to only focus on nights with at least 10 *E. serotinus* passes. We then chose that the biological metric used to define the timing of activity would be the time of the median *E. serotinus* pass during the first half of the night (from 30 min before sunset to 4 h and 30 min after sunset).

We checked that the 10 passes threshold was a sensible choice by resampling the *E. serotinus* passes of the 100 nights with the most *E. serotinus* passes of our dataset (from 61 *E. serotinus* passes to 412). We followed procedure described in Fig. B.1. and drew the Fig. B.2. that synthesise the results obtained according to the number of passes considered. According to the generalised additive model (GAM) fitted to the data, for a 10 passes threshold, the predicted difference between the real median during the first half of the night and the calculated one would be of 5%, which made it a sensible threshold. For instance, the mean value of the median time for these 100 nights is 1 h 43 min 55 s, an incertitude of 5 % would hence be equal to 5 min 12 sec. Furthermore, we calculated the benefit in precision obtained when adding one more *E. serotinus* pass (Fig. B.3.). According to the GAM fitted to the data, when using 11 *E. serotinus* passes instead of 10, we only had a benefit in precision of about 1.75% (for the mean time of the median – 1 h 43 min 55 s – of these 100 nights, it would correspond of a benefit in precision of 1 min 49 s) and this benefit kept on decreasing when the number of passes considered increased.

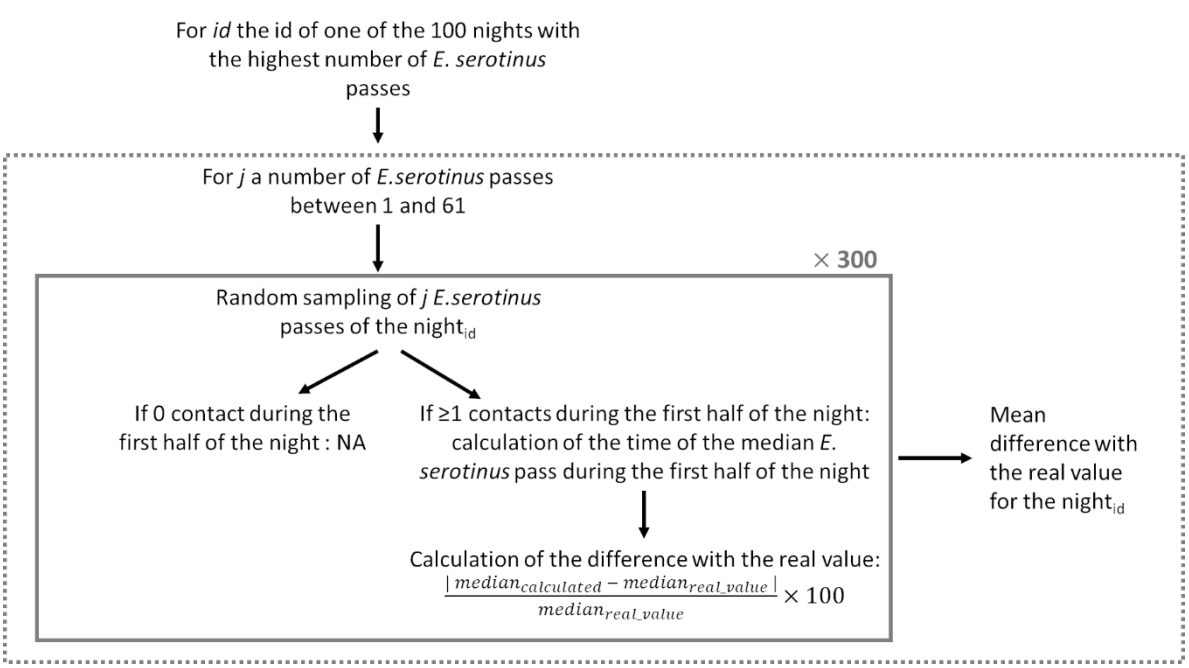

Fig. B.1: Resampling procedure followed to check how many samples are needed for the timing of the median pass during the first half of the night to stabilize.

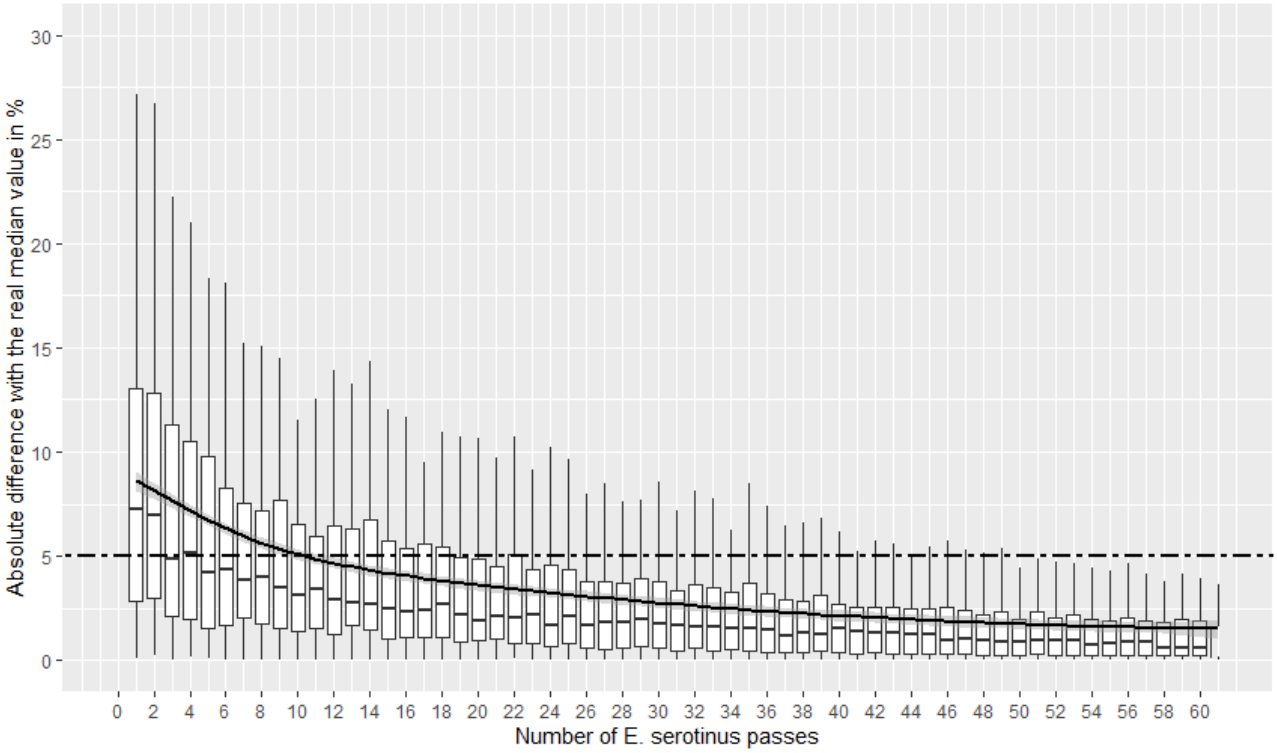

Fig. B.2.: Boxplots synthesizing the mean difference between the known value of the median during the first half of the night and the calculated one after resampling according to a given

number of *E. serotinus* passes 300 times (for the 100 nights with the highest number of *E. serotinus* passes). The solid curve represents the result of a GAM fitted to the data. The dashed line represents a 5% threshold for the absolute difference with the real median value.

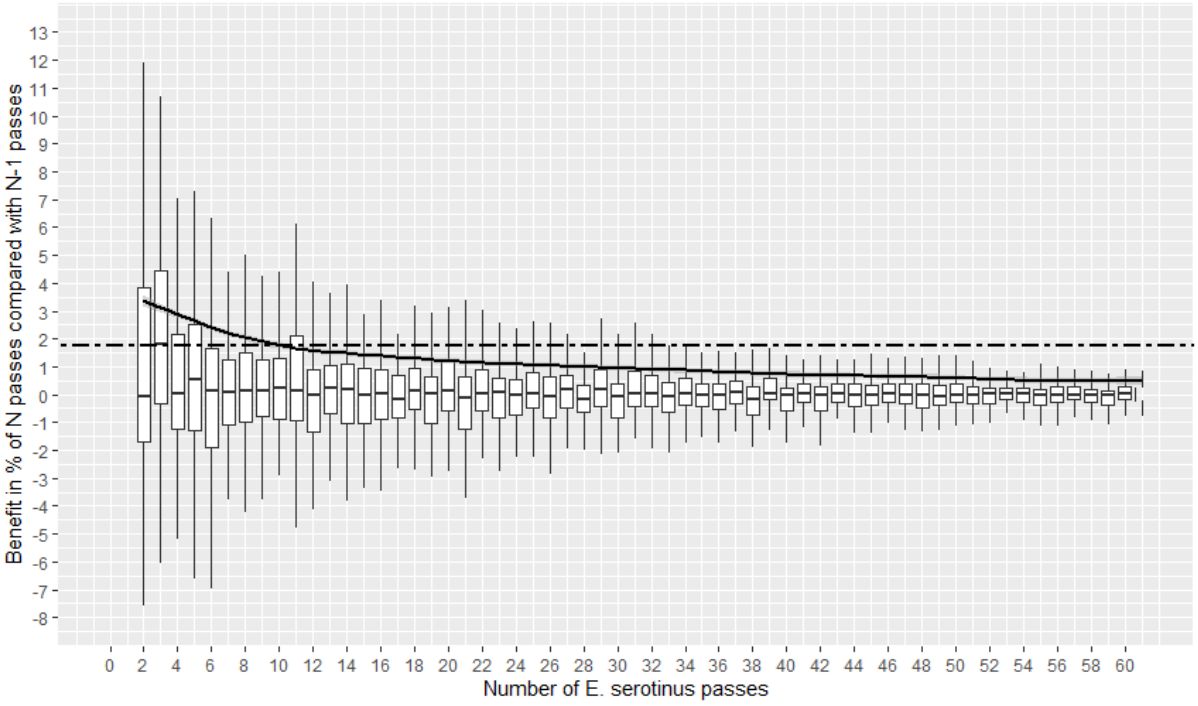

Fig. B.3.: Boxplots synthesizing the benefit in precision obtained when adding one more *E. serotinus* pass. The solid curve represents the result of a GAM fitted to the data. The dashed line represents a benefit of 1.75% in precision when adding one more *E. serotinus* pass.

Supplementary material C: Comparison of the French radiance gradient with the radiance gradient in our datasets

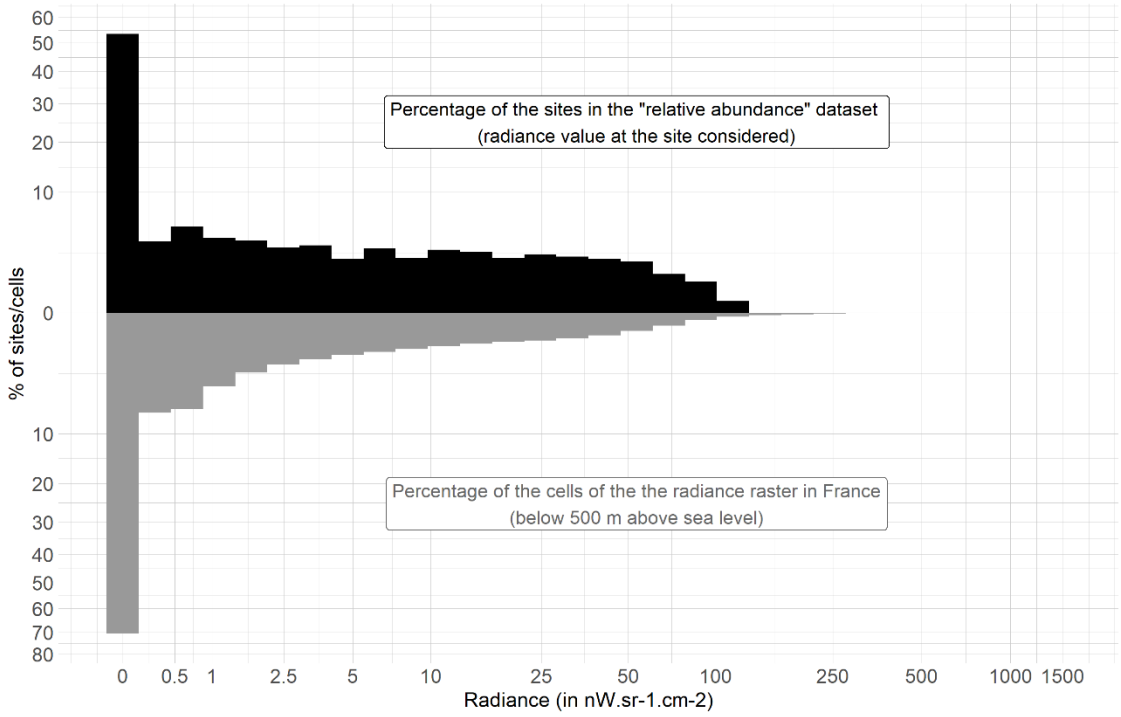

Fig. C.1: Comparison of the French radiance gradient (radiance values of each raster cell of the VIIRS in France, which is below 500 m above sea level) with the radiance gradient of the studied sites in the "relative abundance" dataset (the radiance value considered is the radiance of the raster cell in which the site is located).

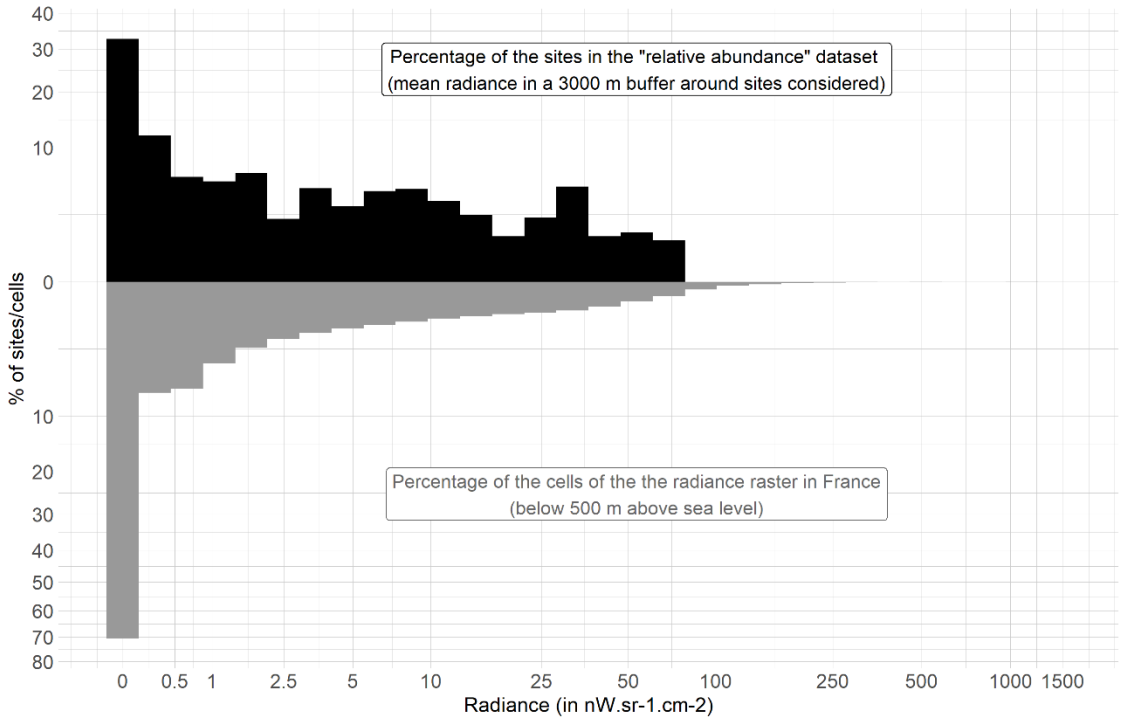

Fig. C.2: Comparison of the French radiance gradient (radiance values of each cell of the VIIRS in France, which is below 500 m above sea level) with the radiance gradient of the studied sites in the "relative abundance" dataset (the radiance value considered is the mean radiance value across 3000 m buffer zones around sites).

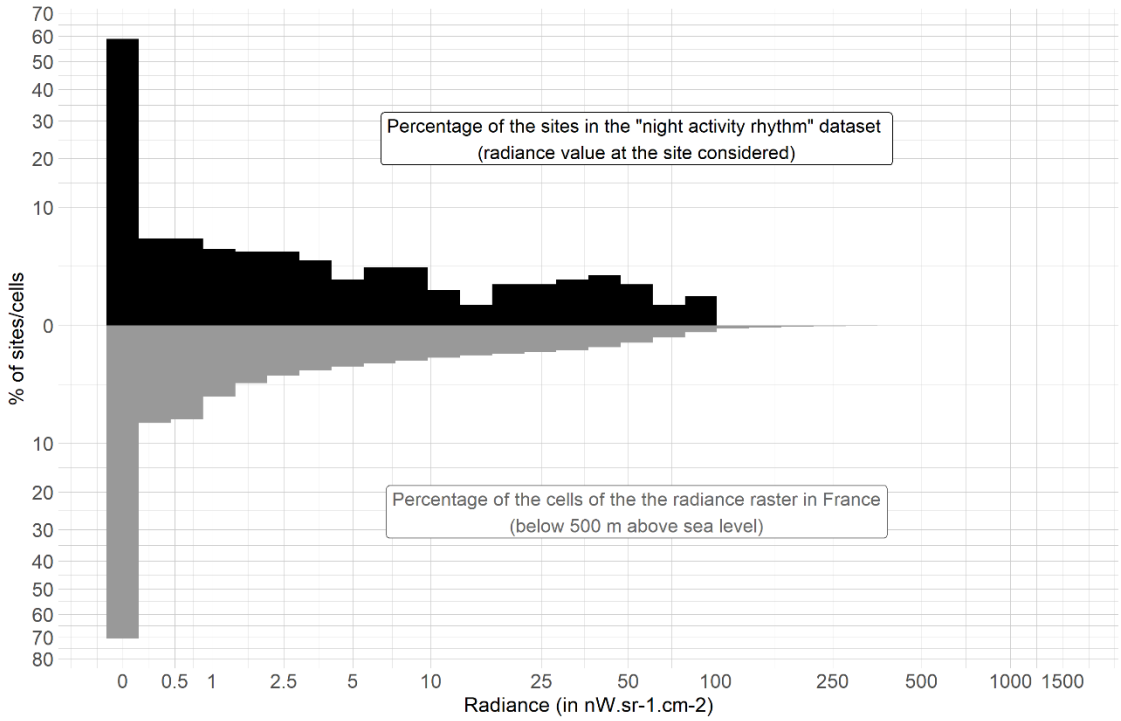

Fig. C.3: Comparison of the French radiance gradient (radiance values of each cell of the VIIRS in France, which is below 500 m above sea level) with the radiance gradient of the studied sites in the "timing of activity" dataset (the radiance value considered is the radiance of the raster cell in which the site is located).

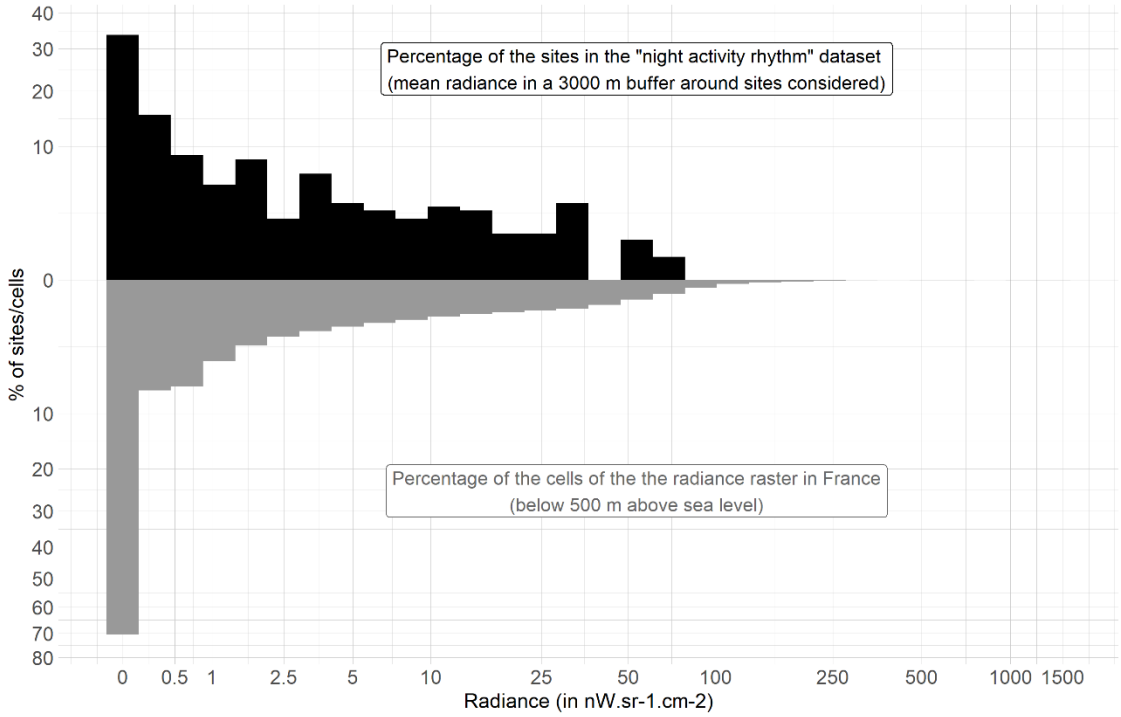

Fig. C.4: Comparison of the French radiance gradient (radiance values of each cell of the VIIRS in France, which is below 500 m above sea level) with the radiance gradient of the studied sites in the “timing of activity” dataset (the radiance value considered is the mean radiance value across 3000 m buffer zones around sites).

Supplementary material D: Influence of the spatial scale at which the ALAN metric is calculated

1. *Heterogeneity across 3000 m buffer zones*

In this study, we hypothesised that bat spatiotemporal distribution might not only be impacted by light pollution levels at the recorder sites but more generally by light pollution at a larger spatial scale, similar to the scale of their vital domain. For example, if a roost is located in a light-polluted area, bats may emerge later from it and arrive later to their foraging sites whether they are light-polluted or dark. Such delay may then result in a reduced efficient time-budget to forage (i.e., a reduced time period during which bats may forage on the prey their diets are mainly composed of) with potential consequences on individual fitness, population dynamics and, *in fine*, bat abundance. Thus, we chose to focus on light pollution at landscape scale so that the metric would include light pollution within the whole *E. serotinus* vital domain and not only where the recordings were carried out. To do so, we considered buffer zones with a radius of 3000 m around sites, as it covered the mean distance between foraging sites and roosts (Catto et al., 1996; Kervyn, 2001; Robinson & Stebbings, 1997).

We measured radiance (i.e., ALAN) heterogeneity in the 3000 m buffer zones around sites by calculating standard deviations and coefficients of variation across them. The higher the mean radiance in the 3000 m buffer zones around sites, the higher was the standard deviation but the lower was the coefficient of variation in the buffer zones (see Table D.1 for a summary of these metrics for both dataset and Fig. D.1 and D.2 for graphic representations).

Despite some heterogeneity in the buffer zones, the Pearson Correlation Coefficients (PCC) between the mean radiance in the 3000 m buffer zones around sites and the radiance at the sites were high (PCC = 0.87 for the “relative abundance” dataset and PCC = 0.86 for the

"timing of activity" dataset). Such correlations suggested that generally, the radiance at the recorder sites was representative of the radiance in the buffer zones around sites.

Table D.1.: Number of raster cells, mean radiance, standard deviance and coefficient of variation in the 3000 m buffer zones around sites. The coefficient of variation is equal to 0 if the mean radiance and the standard deviation are equal to 0, to standard deviation divided by mean radiance otherwise.

	Number of cells	Mean radiance	Standard deviation	Coefficient of variation
Relative abundance dataset	**mean: 229.2** (min:225; max: 232)	**mean: 6.34** (min:0; max: 74.1)	**mean: 4.7** (min:0; max: 36.7)	**mean: 2.4** (min:0; max: 15.2)
Timing of activity dataset	**mean: 229.3** (min:225; max: 232)	**mean: 4.1** (min:0; max: 62.0)	**mean: 3.8** (min:0; max: 24.4)	**mean: 2.6** (min:0; max: 15.1)

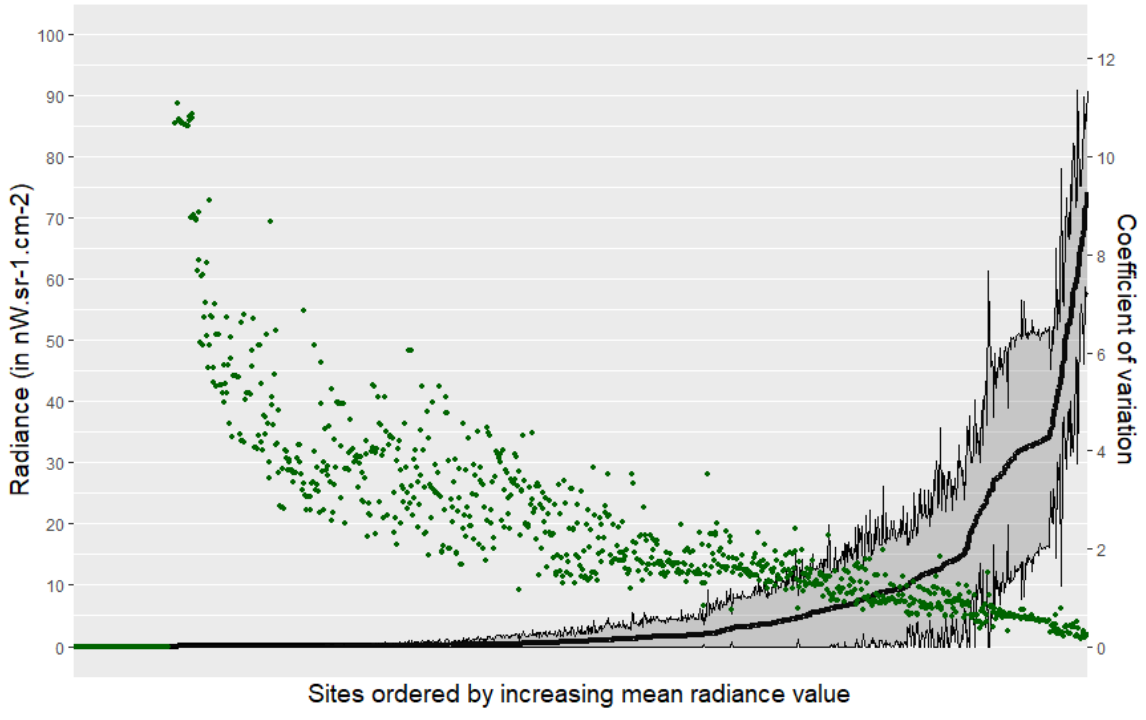

Fig. D.1: Radiance variation in each 3000 m buffer zone for the "relative abundance" dataset. Sites are ordered by increasing mean radiance value, this value being represented by the solid line. The grey ribbon upper limit corresponds to the mean radiance value in the buffer zone

plus the standard deviation in the buffer zone. The lower limit is equal to zero if the mean radiance is lower than the standard deviation, and to the mean radiance minus the standard deviation otherwise. The green dots represent the coefficient of variance of the radiance in each 3000 m buffer zone (equal to 0 if the mean radiance and the standard deviation in the buffer are equal to 0).

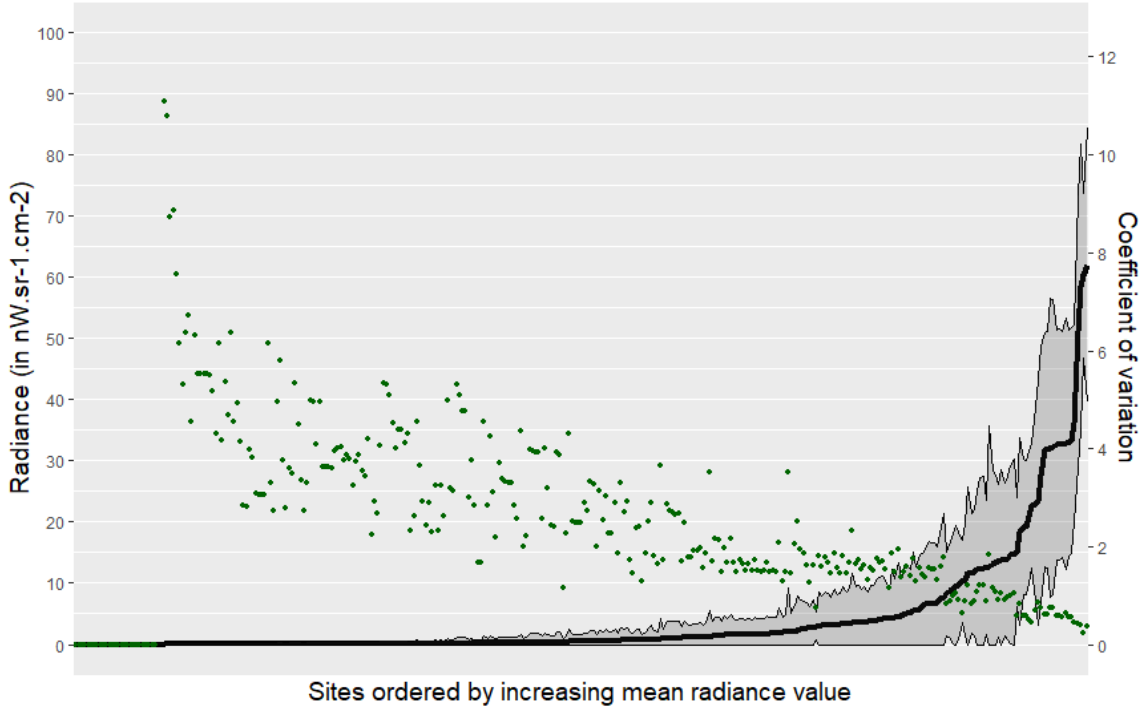

Fig. D.2: ALAN variation in each 3000 m buffer zone for the "timing of activity" dataset. Sites are ordered by increasing mean radiance value, this value being represented by the solid line. The grey ribbon upper limit corresponds to the mean radiance value in the buffer zone plus the standard deviation in the buffer zone. The lower limit is equal to zero if the mean radiance is lower than the standard deviation, and to the mean radiance minus the standard deviation otherwise. The green dots represent the coefficient of variance of the radiance in each 3000 m buffer zone (equal to 0 if the mean radiance and the standard deviation within the buffer are equal to 0).

301 *2. Analyses with the ALAN value at the recorder sites*

302 We carried the same analyses as those presented in the main text, but with the ALAN value of
303 the VIIRS raster cell (~351 m * 351 m) in which the sites were, instead of the mean ALAN
304 value in 3000 m buffer zones around sites.

305 Interestingly for both the "relative abundance" and "timing of activity" analyses, the
306 AICc (second order bias correction for Akaike Information Criterion) was lower when
307 considering the mean ALAN value in buffer zones rather than the ALAN value at the sites
308 (Table D.2). For the "relative abundance" analyses, the results with the ALAN value at the
309 sites were quite similar to those obtained with the mean ALAN value in the buffer zones, the
310 same estimates had a 95% confidence interval that did not overlap zero (Table D.3). However,
311 with the ALAN value at the sites, artificialized surfaces had a much higher sum of weights
312 (SW = 0.87) than ALAN (SW = 0.13). For the "timing of activity" analyses, the results with
313 the ALAN value at the sites were quite similar to those obtained with the mean ALAN value
314 in the buffer zones, the same estimates had a 95% confidence interval that did not overlap
315 zero, apart from the interactions (Table D.4). As a matter of fact, when considering the ALAN
316 value at the site, the estimates of the interactions between ALAN and moonlight, and ALAN
317 and cloud cover overlapped zero.

318

Table D.2: Results of the model averaging for the "relative abundance" and the "timing of activity" analyses. Even if a lot of models were selected in these analyses, the differences between the AICc of the null model and the AICc of the best model were always high.

		Number of models in a ΔAICc of 6	AICc of the best model	AICc of the null model	AICc null model* – AICc best model
Relative abundance dataset	ALAN site	128	10,545	10,796	251
	ALAN buffer	373	10,542	10,796	254
Timing of activity dataset	ALAN site	350	27,844	27,991	147
	ALAN buffer	142	27,831	27,991	160

*include the random effects for "relative abundance" and "timing of activity" analyses, include the weight on the logarithm of the number of *E. serotinus* passes for the "timing of activity" analyses.

Table D.3: Model averaging results for a delta AICc of six points for the "relative abundance" analyses: estimate, sum of weights (SW) and 95% confidence interval (CI) for each variable (apart from latitude and recorder type that were fixed) (estimates in bold when the 95% confidence interval did not overlap zero and the SW was above 0.60). Results with the ALAN value at the recorder sites as the ALAN metric and with the mean ALAN value in the 3000 m buffer zones as the ALAN metric are both represented so that they might be compared. All quantitative fixed effects were scaled and estimates were standardized by dividing them by the standard deviation of the response variable.

	With the ALAN value at the sites as the ALAN metric			With mean ALAN value in the 3000 m buffer zones as the ALAN metric		
Variables	Estimates	SW	CI (95%)	Estimates	SW	CI (95%)
Temperature	**0.0100**	1.00	0.005 ; 0.015	**0.0098**	1.00	0.0047 ; 0.0150

Difference_temperature	**0.0110**	1.00	0.007 ; 0.016	**0.0118**	1.00	0.0071 ; 0.0164
Windspeed	-0.0020	0.46	-0.006 ; 0.001	-0.0025	0.47	-0.0060 ; 0.0011
Difference_precipitations	**-0.0060**	1.00	-0.010 ; -0.003	**-0.0061**	1.00	-0.0098 ; -0.0024
Julian_Day	**0.0120**	1.00	0.008 ; 0.017	**0.0124**	1.00	0.0077 ; 0.0171
(Julian_Day)²	-0.0020	0.32	-0.007 ; 0.003	-0.0023	0.32	-0.0072 ; 0.0027
Cloud_cover	0.0030	0.68	-0.001 ; 0.006	0.0026	0.67	-0.0009 ; 0.0061
Artificialized_surfaces	**-0.0160**	0.87	-0.023 ; -0.009	-0.0156	0.11	-0.0227 ; -0.0086
Grassland	-0.0040	0.37	-0.010 ; 0.003	-0.0047	0.50	-0.0114 ; 0.0020
Deciduous_forest	**0.0100**	1.00	0.005 ; 0.016	**0.0096**	1.00	0.0041 ; 0.0151
Conifer_forest	**0.0130**	1.00	0.007 ; 0.020	**0.0124**	1.00	0.0057 ; 0.0192
Habitat_diversity	**0.0090**	1.00	0.003 ; 0.015	**0.0068**	0.82	0.0005 ; 0.0132
Min_distance_freshwater	-0.0030	0.31	-0.010 ; 0.004	-0.0039	0.37	-0.0116 ; 0.0037
Small_woody_features	**0.0090**	1.00	0.003 ; 0.014	**0.0082**	1.00	0.0026 ; 0.0138
ALAN	-0.0140	0.13	-0.020 ; -0.007	**-0.0186**	0.89	-0.0268 ; -0.0104
Moonlight	**-0.0060**	1.00	-0.010 ; -0.002	**-0.0065**	1.00	-0.0105 ; -0.0025
Difference_temperature :Temperature	0.0010	0.27	-0.003 ; 0.005	0.0009	0.24	-0.0026 ; 0.0045
Cloud_cover:Moonlight	0.0020	0.23	-0.002 ; 0.005	0.0015	0.21	-0.0017 ; 0.0047
ALAN:Cloud_cover	0.0010	0.01	-0.004 ; 0.005	-0.0011	0.14	-0.0056 ; 0.0035
Moonlight:ALAN	0.0000	0.01	-0.004 ; 0.005	-0.0006	0.19	-0.0048 ; 0.0036

Table D.4: Model averaging results for a delta AICc of six points for the "timing of activity" analyses: estimate, sum of weights (SW) and 95% confidence interval (CI) for each variable (apart from latitude and the autocovariate that were fixed) (estimates in bold when the 95% confidence interval did not overlap zero and the SW was above 0.60). Results with the ALAN value at the recorder sites as the ALAN metric and with the mean ALAN value in the 3000 m buffer zones as the ALAN metric are both represented so that they might be compared. All quantitative fixed effects were scaled and estimates were standardized by dividing them by the standard deviation of the response variable.

	With the ALAN value at the sites as the ALAN metric			With mean ALAN value in the 3000 m buffer zones as the ALAN metric		
Variables	Estimates	SW	CI (95%)	Estimates	SW	CI (95%)
Temperature	0.034	0.28	-0.044 ; 0.112	0.031	0.31	-0.047 ; 0.110
Difference_temperature	**0.113**	1.00	0.062 ; 0.164	**0.114**	1.00	0.064 ; 0.165
Windspeed	**-0.092**	1.00	-0.135 ; -0.048	**-0.093**	1.00	-0.136 ; -0.050
Difference_precipitations	**-0.051**	0.89	-0.097 ; -0.004	**-0.053**	0.91	-0.099 ; -0.006
Julian_Day	-0.013	1.00	-0.099 ; 0.074	-0.031	1.00	-0.119 ; 0.057
(Julian_Day)²	**0.152**	1.00	0.074 ; 0.231	**0.142**	1.00	0.061 ; 0.223
Cloud_cover	**-0.157**	1.00	-0.201 ; -0.113	**-0.155**	1.00	-0.199 ; -0.110
Artificialized_surfaces	0.169	0.12	0.053 ; 0.285	NA	NA	NA
Grassland	-0.019	0.16	-0.132 ; 0.095	0.012	0.18	-0.111 ; 0.135
Deciduous_forest	-0.077	0.31	-0.205 ; 0.052	-0.059	0.26	-0.189 ; 0.072
Conifer_forest	-0.026	0.18	-0.144 ; 0.092	-0.017	0.18	-0.138 ; 0.104
Habitat_diversity	0.020	0.18	-0.087 ; 0.127	0.017	0.18	-0.090 ; 0.123
Min_distance_freshwater	0.027	0.17	-0.121 ; 0.176	0.041	0.20	-0.107 ; 0.190
Small_woody_features	-0.044	0.25	-0.157 ; 0.068	-0.067	0.36	-0.181 ; 0.047
ALAN	**0.167**	0.88	0.060 ; 0.273	**0.235**	1.00	0.117 ; 0.354
Moonlight	**0.076**	0.99	0.016 ; 0.135	**0.092**	1.00	0.032 ; 0.152
Difference_temperature :Temperature	-0.011	0.04	-0.053 ; 0.031	-0.024	0.09	-0.066 ; 0.019
Cloud_cover:Moonlight	-0.007	0.17	-0.050 ; 0.035	-0.013	0.21	-0.055 ; 0.030
ALAN:Cloud_cover	-0.004	0.14	-0.053 ; 0.046	**0.059**	0.95	0.011 ; 0.106
Moonlight:ALAN	-0.044	0.39	-0.107 ; 0.020	**-0.073**	1.00	-0.12 ; -0.027

In the "relative abundance" analyses, the selection of artificialized surfaces over ALAN when considering ALAN value at local scale might be explained by several mechanisms. First, Azam et al. (2016) showed that *E. serotinus* abundance at landscape scale was negatively impacted by light pollution. However, locally, *E. serotinus* can forage near streetlight to benefit from the high densities of insect they attract (Stone et al., 2015) but at a slighter higher scale (from 25 to 50 m from streetlights) an avoidance behaviour might be

observed (Azam et al., 2018). Hence, we hypothesised that ALAN would reduce *E. serotinus* abundance at landscape scale but we did not have strong hypotheses on what would be the local effect of light pollution on abundance. Furthermore, the mean ALAN value in the 3000 m buffer zones around sites was highly correlated to the ALAN value at the sites (PCC = 0.87 for the "relative abundance" dataset) but also to the percentage of artificialized surfaces in the 3000 m buffer zones (PCC = 0.88). Hence, the artificialized surfaces effect might also reflect the ALAN effect at landscape scale.

In the "timing of activity" analyses, we did not find any effect of the interactions between ALAN and moonlight, and ALAN and cloud cover when we considered the ALAN value at the recording sites. These two interactions were put in the model to evaluate how diffuse light pollution might interact with other environmental factors. Hence, it is not surprising that, when considering light pollution locally, these interactions did not have any effect any more. Moonlight affect the whole landscape (i.e., the whole *E. serotinus* vital domain) and thus, its effect might be weaker if globally there is a high light pollution intensity. Likewise, cloud cover might amplify diffuse light pollution at landscape scale whereas it should not have any effect on the local light pollution level directly created by several localised streetlights.

Bibliography

Azam, C., Le Viol, I., Bas, Y., Zissis, G., Vernet, A., Julien, J.-F., & Kerbiriou, C. (2018). Evidence for distance and illuminance thresholds in the effects of artificial lighting on bat activity. *Landscape and Urban Planning*, *175*, 123–135. https://doi.org/10.1016/j.landurbplan.2018.02.011

Azam, C., Le Viol, I., Julien, J.-F., Bas, Y., & Kerbiriou, C. (2016). Disentangling the relative effect of light pollution, impervious surfaces and intensive agriculture on bat activity with a national-scale monitoring program. *Landscape Ecology*, *31*(10), 2471–2483. https://doi.org/10.1007/s10980-016-0417-3

Catto, C. M. C., Hutson, A. M., Racey, P. A., & Stephenson, P. J. (1996). Foraging behaviour and habitat use of the serotine bat (*Eptesicus serotinus*) in southern England. *Journal of Zoology*, *238*(4), 623–633. https://doi.org/10.1111/j.1469-7998.1996.tb05419.x

Kervyn, T. (2001). *Ecology and ethology of the serotine bat, Eptesicus serotinus (Chiroptera, Vespertilionidae): Perspectives for the conservation of bats*. University of Liège.

Robinson, M. F., & Stebbings, R. E. (1997). Activity of the serotine bat, *Eptesicus serotinus*. *Myotis*, *35*, 5–16.

Stone, E. L., Harris, S., & Jones, G. (2015). Impacts of artificial lighting on bats: A review of challenges and solutions. *Mammalian Biology*, *80*(3), 213–219. https://doi.org/10.1016/j.mambio.2015.02.004

Supplementary material E: Details the calculation and selection of environmental variables

1. Moonlight

We included moonlight by extracting moon illumination at 9 PM (in %) (R package, *lunar*) and moonrise (R package *suncalc*) for each surveyed night. We then computed the following synthesis variable:

$$Moonlight = Moon\_illumination \times Moonrise\_bin \quad \text{Eq. (E.1)}$$

With:

Moon_illumination: moon illumination (in %) at 9 PM the day when the surveyed night began

Moonrise_bin: equal to zero if moonrise happened after the first 4 h and 30 min after sunset, equal to 1 if moonrise happened before or during the first 4 h and 30 min hours after sunset.

2. Weather

2.1.Calculation of the difference of weather with previous days

The difference of weather with previous days was defined as followed:

$$Weather\_Diff_{Day\ n} = Weather_{Day\ n} - \left(\sum_{i=1}^{5} Weather_{Day\ n-i} \times (6-i)\right)/15 \quad \text{Eq. (E.2)}$$

With:

Weather: Temperature (anomaly), precipitations or windspeed

Day n: Day during which the night began

2.2. Calculation of the temperature and precipitation metrics

To extract temperature (in °C) and precipitation (in mm) data, we used the EObs daily gridded observational dataset for its high temporal (daily data) and spatial resolution (0.1 deg) (Copernicus, https://surfobs.climate.copernicus.eu/dataaccess/access_eobs.php#datafiles, Cornes et al., 2018) (R package *ncdf4*). Each studied site was associated to the grid cell whose centre was closer, and for each night the mean temperature and the sum of precipitations of the day when the night began were extracted.

Absolute measures of temperature may be misleading if *E. serotinus* populations adapt to local climatic conditions: a given temperature may represent a mild day for one population but a cold day for another. We therefore chose to transform temperature in temperature anomalies, defined as followed:

$$Anomaly_{YYYY/MM/DD} = Temperature_{YYYY/MM/DD} - \left(\sum_{i=1980}^{2010} Temperature_{i/MM/DD} \right) /30 \quad \text{Eq. (E.3)}$$

With: *YYYY/MM/DD*: Day during which the surveyed night began (Year: *YYYY*, Month: *MM*, Day: *DD*)

2.3. Calculation of windspeed

For windspeed data, we used R package *RNCEP* (Kemp et al., 2012) to extract data from the NCEP/NCAR Reanalysis dataset (Kalnay et al., 1996). Data spatial resolution was 2.5 deg and we associated each site to the grid cell whose centre was closer. Data temporal resolution was high (6 hours) and we chose to extract data at 6 PM the day when the night began. We extracted the U-Wind Component [East/West] (in $m.s^{-1}$) and the V-Wind Component [North/South] (in m.s-1) and defined windspeed (in $m.s^{-1}$) as followed:

$$Wind\_speed = \sqrt{(U\_wind\_component)^2 + (V\_wind\_component)^2} \quad \text{Eq. (E.4)}$$

2.4. Correlations

The precipitations of the day when the night began and the difference between the precipitations of the day when the night began and previous days (as defined in Eq. (B.2)) were correlated (Pearson Correlation Coefficient (PCC) = 0.62 for the "relative abundance" dataset and PCC = 0.56 for the "timing of activity" dataset), we therefore only kept the difference (it allowed to obtain a better AICc – second order bias correction for Akaike Information Criterion – when used in our full models for the timing of activity).

The windspeed of the day when the night began and the difference between the windspeed of the day when the night began and previous days (as defined in equation (2)) were highly correlated (PCC = 0.77 for the "relative abundance" dataset and PCC = 0.79 for the "timing of activity" dataset), thus we only kept windspeed of the day (it allowed to obtain a better AICc when used in our full models for the timing of activity).

2.5. Weather filter

To avoid exceptional weather conditions, we only selected nights with a windspeed below 12.5 $m.s^{-1}$ and a sum of precipitations below 20 mm on the day when the night began and the five previous days.

3. Land-use

3.1. Landscape representativity

The Vigie-Chiro program was originally design to study population trends for French bats. It should therefore be based on the representativeness of the sample design and, in particular, the representativeness of the habitat distribution in France. Thus, when a volunteer wanted to take part in the "stationary points protocol", he was encouraged to survey sites that were

randomly sampled near a municipality that he chose. However, if he wanted to, he could also choose where he wanted to carry out surveys.

Despite these precautions, the selection of sites might have been driven by unknown criteria, as the closeness to where the volunteers lived. To ensure that it was not an issue for our study, we compared the gradients of proportions of each land-use type in the 3000 m radius buffer zones around the monitored sites with what would have been found if the sites had strictly been randomly selected. To do so, we randomly sampled sites in a square grid (6000 m * 6000 m) in France and removed sites that were above 500 m above sea level (to fit with the altitude filter applied on our datasets). For each of the 12,252 randomly sampled sites, we calculated the proportion of each land-use type in 3000 m buffer zones and compared it with the proportion of each land-use type in the buffer zones around the studied sites of our datasets. Overall, the buffer zones around the sites of our datasets covered the same land-use type gradient as buffer zones around sites randomly selected in France. (Fig. E.1).

3.2.Correlations

Even though road density could be a relevant variable (Claireau et al., 2019), it was not included in the analyses due to multi-collinearity issues: it was correlated with both artificialized surfaces (PCC = 0.68 for the “relative abundance” dataset and PCC = 0.63 for the “timing of activity” dataset) and ALAN (PCC = 0.59 for the “relative abundance” dataset and PCC = 0.50 for the “timing of activity” dataset).

Crops were the most frequent land-use type around sites and also led to multi-collinearity issues: it was correlated with conifer forest (PCC = - 0,66 for the “relative abundance” dataset and PCC = -0.73 for the “timing of activity” dataset). As land-use impacts on bat abundance and timing of activity was not the focus of this study, we chose not to

consider crops. However, we kept in mind that other habitat effects might reflect those of this land-use type.

ALAN and artificialized surfaces were highly correlated (PCC = 0.88 for the "relative abundance" dataset, PCC = 0.83 for the "timing of activity" dataset).

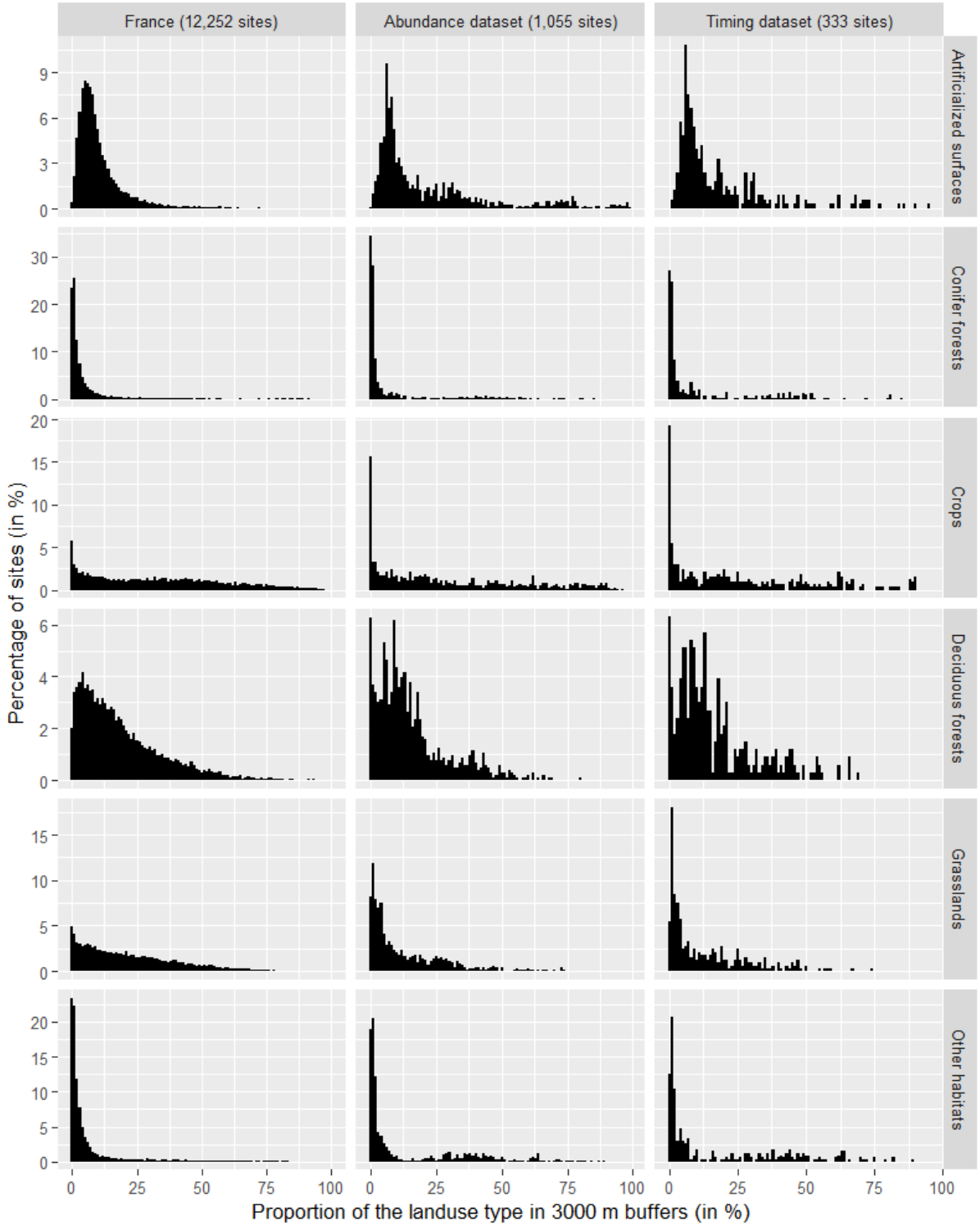

519 Fig E.1: Gradients of proportions of each land-use type in 3000 m buffer zones around
520 randomly sampled sites in France (every 6000 m), the sites of the "relative abundance"
521 dataset and the sites of the "timing of activity" dataset.

522 *Bibliography*

523 Claireau, F., Bas, Y., Pauwels, J., Barré, K., Machon, N., Allegrini, B., Puechmaille, S. J., &
524 Kerbiriou, C. (2019). Major roads have important negative effects on insectivorous bat
525 activity. *Biological Conservation*, *235*, 53–62.
526 https://doi.org/10.1016/j.biocon.2019.04.002
527 Cornes, R. C., van der Schrier, G., van den Besselaar, E. J. M., & Jones, P. D. (2018). An
528 Ensemble Version of the E-OBS Temperature and Precipitation Data Sets. *Journal of*
529 *Geophysical Research: Atmospheres*, *123*(17), 9391–9409.
530 https://doi.org/10.1029/2017JD028200
531 Kalnay, E., Kanamitsu, M., Kistler, R., Collins, W., Deaven, D., Gandin, L., Iredell, M., Saha,
532 S., White, G., Woollen, J., Zhu, Y., Chelliah, M., Ebisuzaki, E., Higgins, W.,
533 Janowiak, J., Mo, K. C., Ropelewski, C., Wang, J., Leetmaa, A., … Joseph, D. (1996).
534 The NCEP/NCAR 40-year reanalysis project. *Bulletin of the American Meteorological*
535 *Society*, *77*(3), 437–472.
536 Kemp, M. U., Emiel van Loon, E., Shamoun-Baranes, J., & Bouten, W. (2012). RNCEP:
537 Global weather and climate data at your fingertips: *RNCEP*. *Methods in Ecology and*
538 *Evolution*, *3*(1), 65–70. https://doi.org/10.1111/j.2041-210X.2011.00138.x

539

Supplementary material F: Gradient of cloud cover for the studied nights

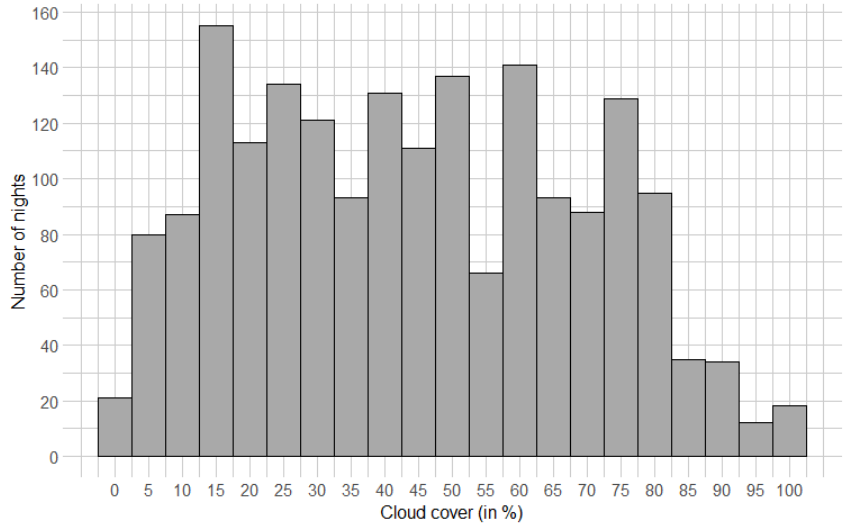

Fig. F.1: Gradient of cloud cover (in %) for the studied nights of the "relative abundance" dataset.

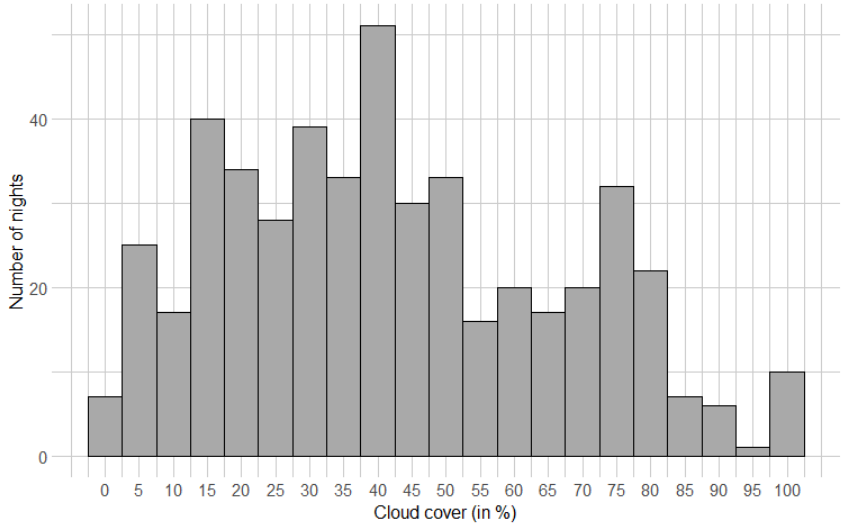

Fig. F.2: Gradient of cloud cover (in %) for the studied nights of the "timing of activity" dataset.

Supplementary material G: Gradient of moonlight for the studied nights

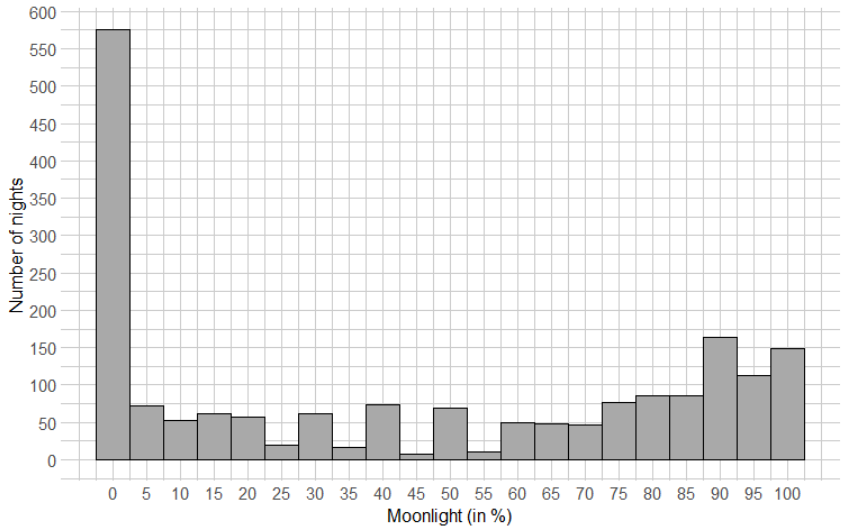

Fig. G.1: Gradient of moonlight for the studied nights of the "relative abundance" dataset. The high number of zeros is explained by the construction of the metric, which was equal to moon illumination (in %) if moonrise happened before the first 4 h and 30 min after sunset during the studied night and zero otherwise.

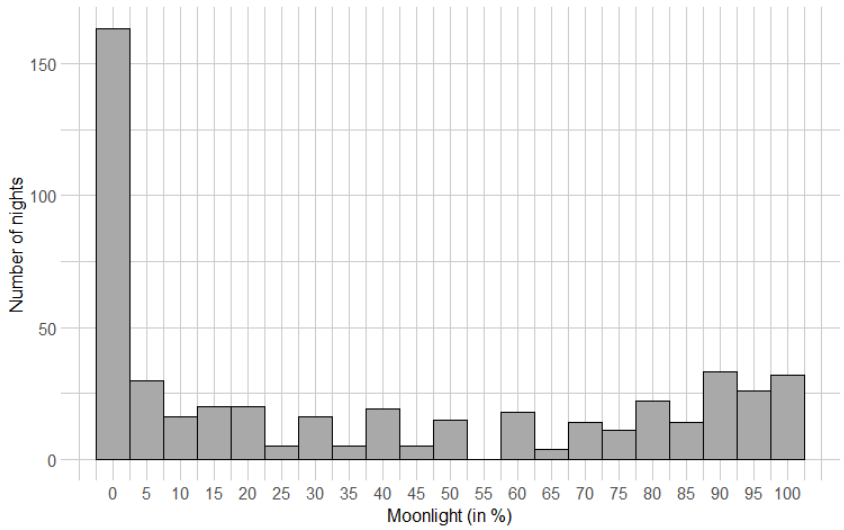

Fig. G.2: Gradient of moonlight for the studied nights of the "timing of activity" dataset. The high number of zeros is explained by the construction of the metric, which was equal to moon illumination (in %) if moonrise happened before the first 4 h and 30 min after sunset during the studied night and zero otherwise.

582 **Table H: Variables extracted to control exogenous factors that could impact *E. serotinus***
583 **relative abundance and timing of activity at their foraging site. The variables that have**
584 **been discarded due to multi-collinearity issues are in brackets. Ab = "relative**
585 **abundance" dataset, Ta = "timing of activity" dataset.**
586

Variable	Mean (Min / Max)	Units	Description	References	Data source
Light pollution					
ALAN	***Ab*** 0.55 (0.00 / 74.12) ***Ta*** 0.38 (0.00 / 62.98)	$nW.sr^{-1}.cm^{-2}$	Mean radiance	/	VIIRS DNB (a)
Environnemental data					
(Crops)	***Ab*** *0.34 (0.00 / 0.96)* ***Ta*** *0.30 (0.00 / 0.90)*	*%*	*Proportion of rape, cereal plant, protein, soya, sunflower and corn crops (3000 m buffer)*	(Azam et al., 2016)	*CESBIO (b)*
Artificialized surfaces	***Ab*** 0.22 (0.00 / 0.97) ***Ta*** 0.18 (0.01 / 0.93)	%	Proportion of dense and diffuse impervious surface, industrial and commercial estates (3000 m buffer)	(Azam et al., 2016)	CESBIO (b)
Conifer forest	***Ab*** 0.06 (0.00 / 0.85) ***Ta*** 0.09 (0.00 / 0.85)	%	Proportion of conifer forest (3000 m buffer)	/	CESBIO (b)
Deciduous forest	***Ab*** 0.14 (0.00 / 0.80) ***Ta*** 0.16 (0.00 / 0.69)	%	Proportion of deciduous forest (3000 buffer m)	(Boughey et al., 2011; Robinson & Stebbings, 1997b)	CESBIO (b)
Grasslands	***Ab*** 0.13 (0.00 / 0.74) ***Ta*** 0.12 (0.00 / 0.74)	%	Proportion of grasslands (3000 m buffer)	(Boughey et al., 2011; Catto et al., 1996; Robinson & Stebbings, 1997b; Vaughan et al., 1997)	CESBIO (b)
(Road density)	***Ab*** *2.30 (0.22 / 8.93)* ***Ta*** *2.07 (0.25 / 8.13)*	*km^{-1}*	*Road density (3000 m buffer)*	*(Claireau et al., 2019)*	*ROUTE 500 ® (c)*
Habitat diversity	***Ab*** 1.74 (0.67 / 2.48)	/	Shannon's diversity index describing habitat	/	CESBIO (b)

	Ta 1.74 (0.67 / 2.45)		diversity (R package *landscapemetrics*) (3000 m buffer)		
Small woody features density	***Ab*** 0.04 (0.00 / 0.17) ***Ta*** 0.04 (0.00 / 0.16)	km^{-1}	Linear and patchy structures of trees, hedges, bushes and scrubs density (3000 m buffer)	(Lacoeuilhe et al., 2016; Verboom & Huitema, 1997)	Copernicus [(d)]
Minimum distance from freshwater	***Ab*** 945 (0 / 6404) ***Ta*** 949 (0.00 / 4887)	km	Minimum distance from lakes and watercourses	(Vaughan et al., 1997)	BD Carthage [(e)]
Meteorological and stronomical data					
Temperature anomaly	***Ab*** 1.27 (-5.99 / 9.34) ***Ta*** 1.97 (-5.26 / 9.34)	°C	Mean temperature anomaly for the day when the night began	(Catto et al., 1995; Vaughan et al., 1997)	EObs [(f)]
Difference temperature anomalies	***Ar*** 0.48 (-7.74 / 7.25) ***Ta*** 1.20 (-4.99 / 7.25)	°C	Difference in anomalies between the day when the night began and the five previous days	(Catto et al., 1995)	EObs [(f)]
Precipitations	***Ab*** *1.29 (0.00 / 19.50)* ***Ta*** *0.66 (0.00 / 12.8)*	*mm*	*Sum of precipitations the day the night began*	*(Catto et al., 1996)*	*EObs [(f)]*
Difference precipitations	***Ab*** -0.40 (-12.30 / 19.32) ***Ta*** -0.67 (-8.90 / 12.28)	mm	Difference in precipitations between the day when the night began and the five previous days	/	EObs [(f)]
Windspeed	***Ab*** 5.50 (0.41 / 12.35) ***Ta*** 5.38 (0.57 / 12.30)	$m.s^{-1}$	Windspeed at 6 PM the day when the night began	(Catto et al., 1996)	NCEP/NCAR Reanalysis [(g)]
Difference windspeed	***Ab*** *-0.30 (-7.57 / 9.40)* ***Ta*** *-0.40 (-7.57 / 9.40)*	*$m.s^{-1}$*	*Difference in win speed between the day when the night began and the five previous days*	/	*NCEP/NCAR Reanalysis [(g)]*
Cloud cover	***Ab*** 44.23 (0.00 / 100) ***Ta*** 42.18 (0.00 / 100)	%	Cloud cover at 6 PM the day when the night began	(Kyba et al., 2015; McAney & Fairley, 1988)	NCEP/NCAR Reanalysis [(g)]
Moonlight	***Ab*** 0.43 (0.00 / 1.00) ***Ta*** 0.37 (0.00 / 1.00)	%	Equal to 0 if no moon in the first 4 h 30 min after sunset, equal to moon illumination otherwise	(Appel et al., 2017; Kolkert et al., 2020; Lang et al., 2006)	R packages *suncalc* and l*unar*

Others					
Julian day	***Ab*** 153 (121 / 171) ***Ta*** 155 (122 / 171)	/	Julian day of the day when the night began	(Catto et al., 1995; Robinson & Stebbings, 1997a)	/
Latitude	***Ab*** 46.41 (41.92 / 50.65) ***Ta*** 46.37 (42.52 / 50.41)	°	Latitude of the monitored site	/	/
Recorder type	/	/	Type of recorder used	/	/

587

588 [(a)] EOG, https://eogdata.mines.edu/products/vnl/

589 [(b)] OSO, http://osr-cesbio.ups-tlse.fr/oso/

590 [(c)] IGN, https://geoservices.ign.fr/documentation/diffusion/telechargement-donnees-

591 libres.html#route-500

592 [(d)] Copernicus, https://land.copernicus.eu/pan-european/high-resolution-layers/small-woody-

593 features/small-woody-features-2015

594 [(e)] IGN, https://geo.data.gouv.fr/fr/datasets/fa9cd96748649d68b59c2a65ebe78258dec4ceeb

595 [(f)] Copernicus, https://surfobs.climate.copernicus.eu/dataaccess/access_eobs.php#datafiles

596 [(g)] Kalnay et al., 1996, extracted with R package *RNCEP* (Kemp et al., 2012)

597

598 *Bibliography*

599 Appel, G., López-Baucells, A., Magnusson, W. E., & Bobrowiec, P. E. D. (2017). Aerial
600 insectivorous bat activity in relation to moonlight intensity. *Mammalian Biology*, *85*,
601 37–46. https://doi.org/10.1016/j.mambio.2016.11.005
602 Azam, C., Le Viol, I., Julien, J.-F., Bas, Y., & Kerbiriou, C. (2016). Disentangling the relative
603 effect of light pollution, impervious surfaces and intensive agriculture on bat activity
604 with a national-scale monitoring program. *Landscape Ecology*, *31*(10), 2471–2483.
605 https://doi.org/10.1007/s10980-016-0417-3
606 Boughey, K. L., Lake, I. R., Haysom, K. A., & Dolman, P. M. (2011). Effects of landscape-
607 scale broadleaved woodland configuration and extent on roost location for six bat

608 species across the UK. *Biological Conservation*, *144*(9), 2300–2310.
609 https://doi.org/10.1016/j.biocon.2011.06.008
610 Catto, C. M. C., Hutson, A. M., Racey, P. A., & Stephenson, P. J. (1996). Foraging behaviour
611 and habitat use of the serotine bat (*Eptesicus serotinus*) in southern England. *Journal*
612 *of Zoology*, *238*(4), 623–633. https://doi.org/10.1111/j.1469-7998.1996.tb05419.x
613 Catto, C. M. C., Racey, P. A., & Stephenson, P. J. (1995). Activity patterns of the serotine bat
614 (*Eptesicus serotinus*) at a roost in southern England. *Journal of Zoology*, *235*(4), 635–
615 644. https://doi.org/10.1111/j.1469-7998.1995.tb01774.x
616 Claireau, F., Bas, Y., Pauwels, J., Barré, K., Machon, N., Allegrini, B., Puechmaille, S. J., &
617 Kerbiriou, C. (2019). Major roads have important negative effects on insectivorous bat
618 activity. *Biological Conservation*, *235*, 53–62.
619 https://doi.org/10.1016/j.biocon.2019.04.002
620 Kalnay, E., Kanamitsu, M., Kistler, R., Collins, W., Deaven, D., Gandin, L., Iredell, M., Saha,
621 S., White, G., Woollen, J., Zhu, Y., Chelliah, M., Ebisuzaki, E., Higgins, W.,
622 Janowiak, J., Mo, K. C., Ropelewski, C., Wang, J., Leetmaa, A., … Joseph, D. (1996).
623 The NCEP/NCAR 40-year reanalysis project. *Bulletin of the American Meteorological*
624 *Society*, *77*(3), 437–472.
625 Kemp, M. U., Emiel van Loon, E., Shamoun-Baranes, J., & Bouten, W. (2012). RNCEP:
626 Global weather and climate data at your fingertips: *RNCEP*. *Methods in Ecology and*
627 *Evolution*, *3*(1), 65–70. https://doi.org/10.1111/j.2041-210X.2011.00138.x
628 Kolkert, H., Smith, R., Rader, R., & Reid, N. (2020). Insectivorous bats foraging in cotton
629 crop interiors is driven by moon illumination and insect abundance, but diversity
630 benefits from woody vegetation cover. *Agriculture, Ecosystems & Environment*, *302*,
631 107068. https://doi.org/10.1016/j.agee.2020.107068
632 Kyba, C. C. M., Tong, K. P., Bennie, J., Birriel, I., Birriel, J. J., Cool, A., Danielsen, A.,
633 Davies, T. W., Outer, P. N. den, Edwards, W., Ehlert, R., Falchi, F., Fischer, J.,
634 Giacomelli, A., Giubbilini, F., Haaima, M., Hesse, C., Heygster, G., Hölker, F., …
635 Gaston, K. J. (2015). Worldwide variations in artificial skyglow. *Scientific Reports*, *5*,
636 8409. https://doi.org/10.1038/srep08409
637 Lacoeuilhe, A., Machon, N., Julien, J.-F., & Kerbiriou, C. (2016). Effects of hedgerows on
638 bats and bush crickets at different spatial scales. *Acta Oecologica*, *71*, 61–72.
639 https://doi.org/10.1016/j.actao.2016.01.009

Lang, A. B., Kalko, E. K. V., Römer, H., Bockholdt, C., & Dechmann, D. K. N. (2006). Activity levels of bats and katydids in relation to the lunar cycle. *Oecologia*, *146*, 659–666. https://doi.org/10.1007/s00442-005-0131-3

McAney, C. M., & Fairley, J. S. (1988). Activity patterns of the lesser horseshoe bat *Rhinolophus hipposideros* at summer roosts. *Journal of Zoology*, *216*(2), 325–338. https://doi.org/10.1111/j.1469-7998.1988.tb02433.x

Robinson, M. F., & Stebbings, R. E. (1997a). Activity of the serotine bat, *Eptesicus serotinus*. *Myotis*, *35*, 5–16.

Robinson, M. F., & Stebbings, R. E. (1997b). Home range and habitat use by the serotine bat, *Eptesicus serotinus*, in England. *Journal of Zoology*, *243*(1), 117–136. https://doi.org/10.1111/j.1469-7998.1997.tb05759.x

Vaughan, N., Jones, G., & Harris, S. (1997). Habitat Use by Bats (Chiroptera) Assessed by Means of a Broad-Band Acoustic Method. *The Journal of Applied Ecology*, *34*(3), 716–730. https://doi.org/10.2307/2404918

Verboom, B., & Huitema, H. (1997). The importance of linear landscape elements for the pipistrelle *Pipistrellus pipistrellus* and the serotine bat *Eptesicus serotinus*. *Landscape Ecology*, *12*, 117–125. https://doi.org/10.1007/BF02698211

Supplementary material I: Checks of model assumptions

Model assumptions were tested according to the following procedure: multicollinearity was tested with R package *performance* (VIF below five for each variable and mean VIF below two), spatial and temporal autocorrelations were tested with R package *DHARMa,* QQ-plots were also drawn to assess if distribution choices were sensible. For "timing of activity" analyses, homoscedasticity was assessed with R package *performance*. For "relative abundance" analyses, we plotted standardized residuals against model predictions and controlled zero inflation with R package *DHARM*.

Supplementary material J: Analyses when considering full models without interactions including ALAN

1. Relative abundance

When we did not consider interactions including ALAN, ALAN still was a better predictor of *E. serotinus* relative abundance as its sum of weights (SW) was equal to 0.84 (it was in 73.6% of the models of the model set), compared to artificialized surfaces whose SW was equal to 0.16 (it was in 26.4% of the models of the model set) (Table J.1) (see Table J.2 for details on the model averaging results). Both ALAN and artificialized surfaces estimates were negative, with ALAN one being even lower (-0.0186) than the artificialized surfaces one (-0.0156).

Table J.1: Model averaging results for a delta AICc of six points for the "relative abundance" analyses: estimate, sum of weights (SW) and 95% confidence interval (CI) for each variable (apart from latitude and recorder type that were fixed) (estimates in bold when the 95% confidence interval did not overlap zero and the SW was above 0.60). Results without and with interactions including ALAN are represented so that they might be compared. All quantitative fixed effects were scaled and estimates were standardized by dividing them by the standard deviation of the response variable

	Without interactions including ALAN			With interactions including ALAN		
Variables	Estimates	SW	CI (95%)	Estimates	SW	CI (95%)
Temperature	**0.0098**	1.00	0.0047 ; 0.0150	**0.0098**	1.00	0.0047 ; 0.0150
Difference_temperature	**0.0117**	1.00	0.0070 ; 0.0164	**0.0118**	1.00	0.0071 ; 0.0164
Windspeed	-0.0025	0.47	-0.0061 ; 0.0011	-0.0025	0.47	-0.0060 ; 0.0011
Difference_precipitations	**-0.0061**	1.00	-0.0097 ; -0.0024	**-0.0061**	1.00	-0.0098 ; -0.0024
Julian_Day	**0.0124**	1.00	0.0076 ; 0.0171	**0.0124**	1.00	0.0077 ; 0.0171

(Julian_Day)²	-0.0023	0.34	-0.0072 ; 0.0026	-0.0023	0.32	-0.0072 ; 0.0027
Cloud_cover	0.0027	0.63	-0.0008 ; 0.0062	0.0026	0.67	-0.0009 ; 0.0061
Artificialized_surfaces	-0.0156	0.16	-0.0227 ; -0.0086	-0.0156	0.11	-0.0227 ; -0.0086
Grassland	-0.0047	0.50	-0.0114 ; 0.0020	-0.0047	0.50	-0.0114 ; 0.0020
Deciduous_forest	**0.0096**	1.00	0.0041 ; 0.0151	**0.0096**	1.00	0.0041 ; 0.0151
Conifer_forest	**0.0124**	1.00	0.0056 ; 0.0191	**0.0124**	1.00	0.0057 ; 0.0192
Habitat_diversity	**0.0070**	0.80	0.0005 ; 0.0134	**0.0068**	0.82	0.0005 ; 0.0132
Min_distance_freshwater	-0.0039	0.37	-0.0115 ; 0.0037	-0.0039	0.37	-0.0116 ; 0.0037
Small_woody_features	**0.0082**	1.00	0.0026 ; 0.0138	**0.0082**	1.00	0.0026 ; 0.0138
ALAN	**-0.0186**	0.84	-0.0268 ; -0.0104	**-0.0186**	0.89	-0.0268 ; -0.0104
Moonlight	**-0.0064**	1.00	-0.0104 ; -0.0024	**-0.0065**	1.00	-0.0105 ; -0.0025
Difference_temperature :Temperature	0.0009	0.26	-0.0026 ; 0.0045	0.0009	0.24	-0.0026 ; 0.0045
Cloud_cover:Moonlight	0.0015	0.21	-0.0017 ; 0.0048	0.0015	0.21	-0.0017 ; 0.0047
ALAN:Cloud_cover				-0.0011	0.14	-0.0056 ; 0.0035
Moonlight:ALAN				-0.0006	0.19	-0.0048 ; 0.0036

Table J.2: Results of the model averaging for the “relative abundance” and the “timing of activity” analyses without interactions including ALAN. Even if a lot of models were selected in these analyses, the differences between the AICc of the null model and the AICc of the best model were always high.

	Number of models in a ΔAICc of 6	**AICc of the best model**	**AICc of the null model**	**AICc null model* – AICc best model**
Relative abundance	216	10,542	10,796	254
Timing of activity	130	27,840	27,991	151

*include random effects for “relative abundance” and “timing of activity” analyses, include the weight on the logarithm of the number of *E. serotinus* passes for “timing of activity” analyses.

2. Timing of activity

When we did not consider interactions including ALAN, ALAN still was a better predictor of the median time of activity as its SW was equal to 0.997 (it was in 99.2% of the models of the model set), compared to artificialized surfaces whose SW was equal to 0.003 (it was in 0.8% of the models of the model set) (Table J.3) (see Table J.2 for details on the model averaging results). Furthermore, both ALAN and artificialized surfaces estimates were positive, with ALAN one being even greater (0.218) than the artificialized surfaces one (0.171).

Table J.3: Model averaging results for a delta AICc of six points for the “timing of activity” analyses: estimate, sum of weights (SW) and 95% confidence interval (CI) for each variable (apart from latitude and the autocovariate that were fixed) (estimates in bold when the 95% confidence interval did not overlap zero and the SW was above 0.60). Results without and with interactions including ALAN are both represented so that they might be compared. All quantitative fixed effects were scaled and estimates were standardized by dividing them by the standard deviation of the response variable

	Without interactions including ALAN			With interactions including ALAN		
Variables	Estimates	SW	CI (95%)	Estimates	SW	CI (95%)
Temperature	0.042	0.36	-0.037 ; 0.12	0.031	0.31	-0.047 ; 0.110
Difference_temperature	**0.112**	1.00	0.059 ; 0.165	**0.114**	1.00	0.064 ; 0.165
Windspeed	**-0.089**	1.00	-0.133 ; -0.046	**-0.093**	1.00	-0.136 ; -0.050

Difference_precipitations	**-0.052**	0.90	-0.098 ; -0.005	**-0.053**	0.91	-0.099 ; -0.006
Julian_Day	-0.017	1.00	-0.104 ; 0.071	-0.031	1.00	-0.119 ; 0.057
(Julian_Day)²	**0.154**	1.00	0.077 ; 0.231	**0.142**	1.00	0.061 ; 0.223
Cloud_cover	**-0.155**	1.00	-0.199 ; -0.111	**-0.155**	1.00	-0.199 ; -0.110
Artificialized_surfaces	0.171	0.00	0.061 ; 0.28	NA	NA	NA
Grassland	0.004	0.17	-0.115 ; 0.123	0.012	0.18	-0.111 ; 0.135
Deciduous_forest	-0.057	0.26	-0.186 ; 0.072	-0.059	0.26	-0.189 ; 0.072
Conifer_forest	-0.025	0.20	-0.145 ; 0.095	-0.017	0.18	-0.138 ; 0.104
Habitat_diversity	0.023	0.19	-0.082 ; 0.128	0.017	0.18	-0.090 ; 0.123
Min_distance_freshwater	0.031	0.20	-0.116 ; 0.177	0.041	0.20	-0.107 ; 0.190
Small_woody_features	-0.057	0.32	-0.169 ; 0.056	-0.067	0.36	-0.181 ; 0.047
ALAN	**0.218**	1.00	0.102 ; 0.335	**0.235**	1.00	0.117 ; 0.354
Moonlight	**0.076**	0.99	0.016 ; 0.136	**0.092**	1.00	0.032 ; 0.152
Difference_temperature :Temperature	-0.008	0.05	-0.05 ; 0.034	-0.024	0.09	-0.066 ; 0.019
Cloud_cover:Moonlight	-0.008	0.18	-0.05 ; 0.035	-0.013	0.21	-0.055 ; 0.030
ALAN:Cloud_cover				**0.059**	0.95	0.011 ; 0.106
Moonlight:ALAN				**-0.073**	1.00	-0.120 ; -0.027

713

714

715

Supplementary material K: Checking of the robustness of the model averaging results

1. *Comparison between the model averaging approach and the model selection one*

Relative abundance

The best model obtained with the dredge (i.e., the one with the lowest AICc – second order bias correction for Akaike Information Criterion) was the following one:

Relative abundance metric ~ Conifer_forest + Deciduous_forest + Julian_day + Moonlight + Small_woody_features + Habitat_diversity + ALAN + Cloud_cover + Difference_precipitations + Difference_temperature + Temperature + Latitude + Recorder_type + (1 | site / participation) Eq. (K.1)

As shown in Table K.1, the estimates (standardized) of the best model were highly similar to those obtained with the model averaging. The variables that had a sum of weights (SW) above 0.60 and whose 95% interval did not overlap zero were all in the best model and their p-value was significant. Hence, the model averaging and the model selection approaches were consistent. Our conclusions would have been the same whatever the approach chosen.

Table K.1: Comparison between the result obtained with a model selection approach (model with the lowest AICc) and the model averaging approach for the "relative abundance" analyses. In bold, in the column "estimates best model", are the estimates whose p-value was below 0.05 (Anova II). In bold, in the column "estimates model averaging", are the estimate whose SW were above 0.6 and whose 95% confidence interval did not overlap 0. (In this table we did not put latitude and recorder type that were fixed for "relative abundance" analyses).

All quantitative fixed effects were scaled and estimates were standardized by dividing them by the standard deviation of the response variable

Variables	Estimates best model	p-value	Estimates model averaging	SW > 0.60 and 95% interval did not overlap 0
Temperature	**0.0101**	8.7e-05***	**0.0098**	Yes
Difference_temperature	**0.0117**	5.4e-07***	**0.0118**	Yes
Windspeed	NA	NA	-0.0025	No
Difference_precipitations	**-0.0063**	6.9e-04***	**-0.0061**	Yes
Julian_Day	**0.0127**	2.8e-08***	**0.0124**	Yes
(Julian_Day)²	NA	NA	-0.0023	No
Cloud_cover	0.0027	1.2e-01	0.0026	No
Artificialized_surfaces	NA	NA	-0.0156	No
Grassland	NA	NA	-0.0047	No
Deciduous_forest	**0.0101**	1.0e-04***	**0.0096**	Yes
Conifer_forest	**0.0134**	9.8e-06***	**0.0124**	Yes
Habitat_diversity	**0.0074**	1.1e-02*	**0.0068**	Yes
Min_distance_freshwater	NA	NA	-0.0039	No
Small_woody_features	**0.0074**	5.0e-03**	**0.0082**	Yes
ALAN	**-0.0167**	1.5e-06***	**-0.0186**	Yes
Moonlight	**-0.0063**	1.9e-03**	**-0.0065**	Yes
Difference_temperature :Temperature	NA	NA	0.0009	No
Cloud_cover:Moonlight	NA	NA	0.0015	No
ALAN:Cloud_cover	NA	NA	-0.0011	No
Moonlight:ALAN	NA	NA	-0.0006	No

Timing of activity

The best model obtained with the dredge (i.e., the one with the lowest AICc) was the following one:

748 *Timing of activity metric ~ Julian_day + Julian_day² + Moonlight + ALAN + Cloud_cover +*
749 *Difference_precipitations + Difference_temperature + Wind_speed +* Eq. (K.2)
750 *Latitude + autocov + Moonlight : ALAN + ALAN : Cloud_cover + (1 | site)*
751
752 As shown in Table K.2, the estimates (standardized) of the best model were highly
753 similar to those obtained with the model averaging. The covariates that had a sum of weights
754 (SW) above 0.60 and whose 95% interval did not overlap zero were all in the best model and
755 their p-value was significant. Hence, the model averaging and the model selection approaches
756 were consistent. Our conclusions would have been the same whatever the approach chosen.
757
758 Table K.2: Comparison between the result obtained with a model selection approach (model
759 with the best AICc) and the model averaging approach for the "timing of activity" analyses.
760 In bold, in the column "estimates best model", are the estimate whose p-value was below 0.05
761 (Anova II). In bold, in the column "estimates model averaging", are the estimates whose SW
762 were above 0.6 and whose 95% confidence interval did not overlap 0. (In this table we did not
763 put latitude and the autocovariate that were fixed for "timing of activity" analyses). All
764 quantitative fixed effects were scaled and estimates were standardized by dividing them by
765 the standard deviation of the response variable

Variables	Estimates best model	p-value	Estimates model averaging	SW > 0.60 and 95% interval did not overlap 0
Temperature	NA	NA	0.031	No
Difference_temperature	**0.120**	5.6e-08***	**0.114**	Yes
Windspeed	**-0.093**	2.3e-05***	**-0.093**	Yes
Difference_precipitations	**-0.052**	2.4e-02*	**-0.053**	Yes
Julian_Day	-0.027	5.3e-01	-0.031	No
(Julian_Day)²	**0.140**	5.7e-04***	**0.142**	Yes
Cloud_cover	**-0.153**	1.4e-12***	**-0.155**	Yes

Artificialized_surfaces	NA	NA	NA	NA
Grassland	NA	NA	0.012	No
Deciduous_forest	NA	NA	-0.059	No
Conifer_forest	NA	NA	-0.017	No
Habitat_diversity	NA	NA	0.017	No
Min_distance_freshwater	NA	NA	0.041	No
Small_woody_features	NA	NA	-0.067	No
ALAN	**0.233**	1.5e-04***	**0.235**	Yes
Moonlight	**0.092**	8.7e-03**	**0.092**	Yes
Difference_temperature :Temperature	NA	NA	-0.024	No
Cloud_cover:Moonlight	NA	NA	-0.013	No
ALAN:Cloud_cover	**0.058**	1.7e-02*	**0.059**	Yes
Moonlight:ALAN	**-0.074**	1.6e-03**	**-0.073**	Yes

2. Complex model issue

For the model averaging, we chose not to follow Richards et al., (2011) parsimonious approach consisting in post hoc elimination of models that are more complex versions of any model with a lower AICc value. As a matter of fact, it would have been very time-consuming (our model sets were composed of 373 models for the "relative abundance" analyses and 142 models for the "timing of activity" analyses) and, according to Symonds & Moussalli, (2011), it was uncertain if such a method would have consistently improved the model averaging ; whereas Grueber et al. (2011) underlined that some complex models may be composed of unique predictor variables of potentially strong ecological importance that should not be removed in such cases.

Nonetheless, because we did not discard these complex models, there was a risk of overweighting the predictor variables contained in overly complex models. However, as we presented in the first part of this Supplementary materiel (*Comparison between the model*

781 *averaging approach and the model selection one*), for both analyses the best models already
782 contained all the variables for which we found an effect with the model averaging approach.
783 Hence, none of these variables would have been discarded by following Richards et al. (2011)
784 approach.

785 However, Richards et al. (2011) parsimonious approach could potentially change the
786 sum of weights (SW) and confidence interval of these variables. Nonetheless, for the "relative
787 abundance" analyses, almost all variables which had an effect according to our model
788 averaging approach (SW > 0.60 and a 95% confidence interval that did not overlap 0), were in
789 all the models of the models set (373 models) and their p-value was significant in all these
790 models. The exceptions were (1) small woody features but it was in 99.5% of the models and
791 its p-value was significant in all these models; (2) habitat diversity which was a variable that
792 was not discussed in the main text, it had just been added to control potential effect of
793 landscape structure on bat abundance; (3) and ALAN but the models in which this variable
794 was not were those with artificialized surfaces, with no model containing neither of these two
795 variables, ALAN was significant in all the models in which it was included (Table K.3).

796 Likewise, for the "timing of activity" analyses, almost all variables that had effect with
797 our model averaging approach were also included in all the models selected in the model set
798 used for the model averaging and their p-value was significant in all these models. The
799 exceptions were difference of precipitations and the interaction between cloud cover and
800 ALAN, but there were nonetheless in a high percentage of models (respectively 87.3% and
801 92.3%) and their p-values were significant in all the models in which they were included
802 (Table K.4).

803 Moreover, as shown in Fig. K.2 and K.3 of the third part of this Supplementary
804 material (*Multicollinearity effect on coefficient estimates*), the estimates of the variables
805 which had an effect according to our model averaging approach were quite similar in all the

806 models selected in the model set of the model averaging for both analyses. For both analyses,
807 in all the models including ALAN, the absolute value of its estimate was greater than those of
808 the other variables. Hence, we are confident that Richards et al. (2011) approach would have
809 resulted in the same variable selection, in similar estimates, and that ALAN would have
810 stayed the variable whose estimate was the greater in absolute value.
811

Table K.3: Comparison between the obtained results when considering all the models within a ΔAICc of six points individually and the results of the model averaging for the "relative abundance" analyses. In bold are the estimates whose SW were above 0.6 and whose 95% confidence interval did not overlap 0. (In this table we did not put latitude and recorder type that were fixed for "relative abundance" analyses). All quantitative fixed effects were scaled and estimates were standardized by dividing them by the standard deviation of the response variable

Variables	Estimates model averaging	SW > 0.60 and 95% interval did not overlap 0	Percentage of models in the model averaging	Percentage of models in which the p-value is <0.05
Temperature	**0.0098**	**Yes**	**100**	**100**
Difference_temperature	**0.0118**	**Yes**	**100**	**100**
Windspeed	-0.0025	No	48.0	0
Difference_precipitations	**-0.0061**	**Yes**	**100**	**100**
Julian_Day	**0.0124**	**Yes**	**100**	**100**
$(Julian\_Day)^2$	-0.0023	No	40.5	0
Cloud_cover	0.0026	No	71.0	0
Artificialized_surfaces	-0.0156	No	15.3	15.3
Grassland	-0.0047	No	55.5	11.8
Deciduous_forest	**0.0096**	**Yes**	**100**	**100**
Conifer_forest	**0.0124**	**Yes**	**100**	**100**
Habitat_diversity	**0.0068**	**Yes**	**74.5**	**55.5**
Min_distance_freshwater	-0.0039	No	44.2	0
Small_woody_features	**0.0082**	**Yes**	**99.5**	**99.5**
ALAN	**-0.0186**	**Yes**	**84.7**	**84.7**
Moonlight	**-0.0065**	**Yes**	**100**	**100**
Difference_temperature :Temperature	0.0009	No	32.3	0
Cloud_cover:Moonlight	0.0015	No	27.1	0
ALAN:Cloud_cover	-0.0011	No	19.3	0
Moonlight:ALAN	-0.0006	No	26.8	0

Table K.4: Comparison of the obtained results when considering all models within a ΔAICc of six points individually with the results of the model averaging for the "timing of activity" analyses. In bold are the estimate coefficient whose SW were above 0.6 and whose 95% confidence interval did not overlap 0. (In this table we did not put latitude and the autocovariate that were fixed for "timing of activity" analyses). All quantitative fixed effects were scaled and estimates were standardized by dividing them by the standard deviation of the response variable

Variables	Estimates model averaging	SW > 0.60 and 95% interval did not overlap 0	Percentage of models in the model averaging	Percentage of models in which the p-value is <0.05
Temperature	0.031	No	32.3	0
Difference_temperature	**0.114**	**Yes**	**100**	**100**
Windspeed	**-0.093**	**Yes**	**100**	**100**
Difference_precipitations	**-0.053**	**Yes**	**87.3**	**87.3**
Julian_Day	-0.031	No	100	0
$(Julian\_Day)^2$	**0.142**	**Yes**	**100**	**100**
Cloud_cover	**-0.155**	**Yes**	**100**	**100**
Artificialized_surfaces	NA	NA	NA	NA
Grassland	0.012	No	24.6	0
Deciduous_forest	-0.059	No	32.4	0
Conifer_forest	-0.017	No	23.9	0
Habitat_diversity	0.017	No	23.2	0
Min_distance_freshwater	0.041	No	25.4	0
Small_woody_features	-0.067	No	38.7	0
ALAN	**0.235**	**Yes**	**100**	**100**
Moonlight	**0.092**	**Yes**	**100**	**100**
Difference_temperature :Temperature	-0.024	No	11.3	0
Cloud_cover:Moonlight	-0.013	No	26.1	0
ALAN:Cloud_cover	**0.059**	**Yes**	**92.3**	**92.3**
Moonlight:ALAN	**-0.073**	**Yes**	**100**	**100**

3. Multicollinearity effect on coefficient estimates

According to Cade (2015), the presence of multicollinearity leads to different scaling of units for the regression coefficient of a given predictor variable across candidate models with different combinations of predictor variables. To solve this issue and ensure that multimodel inferences are sound, he suggested to standardize estimates based on partial standard deviations.

By excluding predictor variables that were responsible for multicollinearity (difference of windspeed, sum of precipitations of the day, crops, road density) and by never including artificialized surfaces and ALAN in the same models, we ensured that the variance inflation factor (VIF) of our predictor variables and the mean VIF of our models would stay very low. However, Cade (2015) suggested that even when the VIFs are low, there might be changes in the scaling of predictors under different model covariance structures.

Hence, as suggested by Cade (2015), we decided to standardised estimates based on partial standard deviations for their variables. As this method was not implemented in the *model.avg* and the *dredge* functions (R package *MuMIn*) for models fitted with the function glmmTBM (R package *glmmTMB*), we did it by following the procedure shown in Fig. K.1. As shown in Table K.5, Fig. K.2 and Fig. K.3, such standardisation did not change our conclusions: ALAN still was the covariate whose estimate was the highest in absolute value for both analyses. For the “relative abundance” analyses, ALAN estimate was higher than the estimate of artificialized surfaces. Furthermore, even if the standardisation based on partial standard deviation reduced the absolute values of the estimates, their values remained close to those obtained with a “classical” standardisation such as the one used in the main text.

For each covariate (i)

For each model j within a ΔAICc of six points compared to the best model

$$sd_{ij}^{*} = sd_i \sqrt{\frac{1}{VIF_{ij}}} \sqrt{\frac{(n-1)}{(n-p_j)}}$$

sd^{*}: partial standard deviation
sd : standard deviation
VIF : variance inflation factor
n : number of observations
p : number of predictor variables in the model

$$\beta_{ij}^{*} = \beta_{ij} \times sd_{ij}^{*}$$

β^{*} : standardised estimate
β : unstandardised estimate
sd^{*} : partial standard deviation

$Coeff_i^{*}$: standardised estimate of the model averaging
J : number of models in the model averaging
w : weight of the model in the model averaging
SD : standard deviation of the response variable

$$Coeff_i^{*} = \frac{\sum_{j=1}^{J}(\beta_{ij}^{*} \times w_j)}{\sum_{j=1}^{J} wj} \times \frac{1}{SD}$$

Fig. K.1: Procedure followed to standardised estimates based on partial standard deviations in the model averaging (Cade, 2015)

Table K.5: Comparison of the obtained coefficient estimates with the model averaging with a "classical" standardisation of the coefficient estimates and with a standardisation based on partial standard deviations for the "relative abundance" and "timing of activity" analyses (estimates are in bold when the 95% confidence interval did not overlap zero and the SW was above 0.60). (In this table we did not put latitude and recorder type that were fixed for "relative abundance" analyses and latitude and the autocovariate that were fixed for "timing of activity" analyses)

	Relative abundance		Timing of activity	
Variables	Classical	SD partial	Classical	SD partial
Temperature	**0.0098**	**0.0072**	0.031	0.022
Difference_temperature	**0.0118**	**0.0088**	**0.114**	**0.103**
Windspeed	-0.0025	-0.0024	**-0.093**	**-0.089**
Difference_precipitations	**-0.0061**	**-0.0058**	**-0.053**	**-0.051**
Julian_Day	**0.0124**	**0.0114**	-0.031	-0.024
(Julian_Day)²	-0.0023	-0.0020	**0.142**	**0.110**
Cloud_cover	0.0026	0.0025	**-0.155**	**-0.144**
Artificialized_surfaces	-0.0156	-0.0122	NA	NA
Grassland	-0.0047	-0.0037	0.012	0.010
Deciduous_forest	**0.0096**	**0.0082**	-0.059	-0.051
Conifer_forest	**0.0124**	**0.0086**	-0.017	-0.013
Habitat_diversity	**0.0068**	**0.0053**	0.017	0.016
Min_distance_freshwater	-0.0039	-0.0033	0.041	0.041
Small_woody_features	**0.0082**	**0.0069**	-0.067	-0.062
ALAN	**-0.0186**	**-0.0146**	**0.235**	**0.223**
Moonlight	**-0.0065**	**-0.0064**	**0.092**	**0.086**
Difference_temperature :Temperature	0.0009	0.0009	-0.024	-0.022
Cloud_cover:Moonlight	0.0015	0.0015	-0.013	-0.013
ALAN:Cloud_cover	-0.0011	-0.0010	**0.059**	**0.057**
Moonlight:ALAN	-0.0006	-0.0006	**-0.073**	**-0.070**

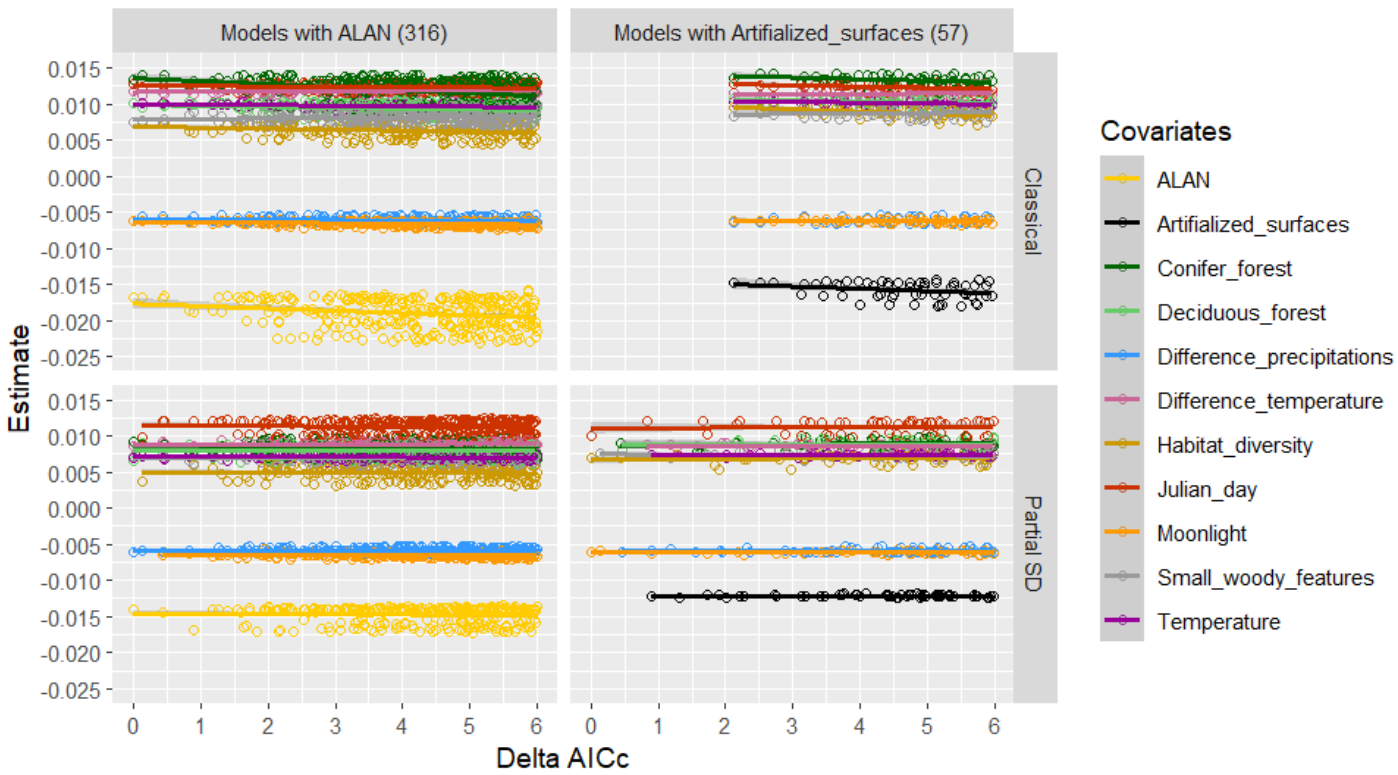

Fig K.2: For the "relative abundance" analyses, variations of the values of the estimates in the 373 models within a ΔAICc of six points compared to the best model. Only the variables which had an effect according to the model averaging approach are represented. Their estimates are represented according to the ΔAICc of the model in which they have been estimated. The solid curves represent the result of generalized linear models fitted to the data. The left panels correspond to all the models in which ALAN was selected and the right panels correspond to all the models in which artificialized surfaces were selected. There was no model with neither ALAN nor artificialized surfaces. The upper panels correspond to "classical" standardised estimates and the lower panels correspond to standardised estimates based on partial standard deviations.

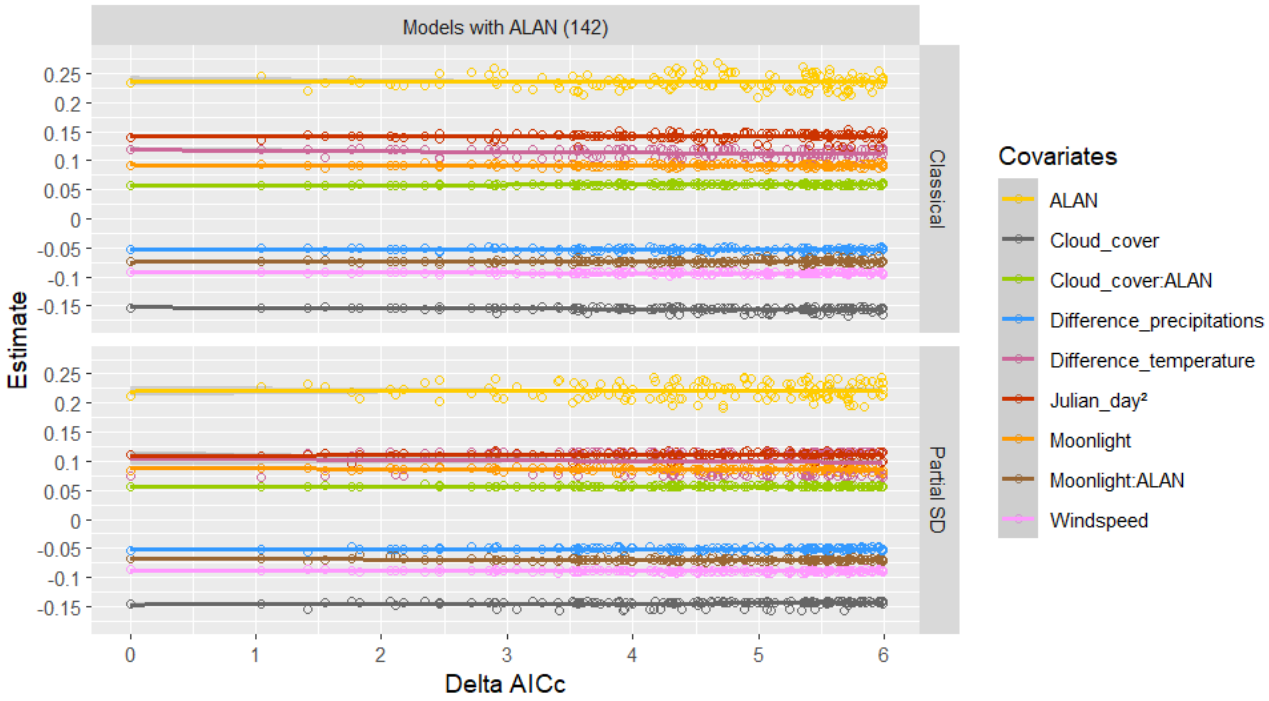

Fig K.3: For the "timing of activity" analyses, variations of the values of the estimates in the 142 models within a ΔAICc of six points compared to the best model. Only the covariates which had an effect according to the model averaging approach are represented. Their estimates are represented according to the ΔAICc of the model in which they have been estimated. The solid curves represent the result of generalized linear models fitted to the data. ALAN was selected over artificialized surfaces in all models. The upper panels correspond to "classical" standardised estimates and the lower panels correspond to standardised estimates based on partial standard deviations.

Bibliography

Cade, B. S. (2015). Model averaging and muddled multimodel inferences. *Ecology*, *96*(9), 2370–2382. https://doi.org/10.1890/14-1639.1

Grueber, C. E., Nakagawa, S., Laws, R. J., & Jamieson, I. G. (2011). Multimodel inference in ecology and evolution: Challenges and solutions: Multimodel inference. *Journal of Evolutionary Biology*, *24*(4), 699–711. https://doi.org/10.1111/j.1420-9101.2010.02210.x

Richards, S. A., Whittingham, M. J., & Stephens, P. A. (2011). Model selection and model averaging in behavioural ecology: The utility of the IT-AIC framework. *Behavioral Ecology and Sociobiology*, *65*(1), 77–89. https://doi.org/10.1007/s00265-010-1035-8

Symonds, M. R. E., & Moussalli, A. (2011). A brief guide to model selection, multimodel inference and model averaging in behavioural ecology using Akaike's information criterion. *Behavioral Ecology and Sociobiology*, *65*(1), 13–21. https://doi.org/10.1007/s00265-010-1037-6

Table L: Results of the model averaging for the "relative abundance" and the "timing of activity" analyses. Even if a lot of models were selected in these analyses, the differences between the AICc of the null model and the AICc of the best model were always high.

	Number of models in a ΔAICc of 6	AICc of the best model	AICc of the null model	AICc null model* – AICc best model
Relative abundance	373	10,542	10,796	254
Timing of activity	142	27,831	27,991	160

*include random effects for "relative abundance" and "timing of activity" analyses, include the weight on the logarithm of the number of *E. serotinus* passes for "timing of activity" analyses.

Table M: Mean of the mean radiances (in nW.sr^{-1}.cm^{-2}) of the French municipalities according to their population size (only municipalities that are below 500 m above sea levels are considered).

Population	Mean of the mean radiances	Number of municipalities
> 900,000	62.83	1 (Paris)
]200,000 ; 900,000]	39.7	10
]50,000 ; 200,000]	35.5	103
]10,000 ; 50,000]	19.6	802
]5000 ; 10,000]	7.8	1122
]1000 ; 5000]	2.2	7446
]500 ; 1000]	0.75	6537
]100 ; 500]	0.35	14,959
< 100	0.24	3458

Fig. N: Interaction between cloud cover and ALAN: Predicted values and 95% confidence intervals of the timing of activity (i.e., the time of the median *E. serotinus* pass during the first half of the night) with all variables equal to zero (i.e,. all variables equal to their mean, as they were previously scaled) apart from cloud cover and ALAN. This graph represents the median time of activity according to cloud cover (back transformed in %) for three values of ALAN (2.2 nW.sr^{-1}.cm^{-2} being the mean radiance of French municipalities of 1000 to 5000 inhabitants and 7.8 nW.sr^{-1}.cm^{-2} being the mean radiance for municipalities of 5000 to 10,000 inhabitants, see Table M).

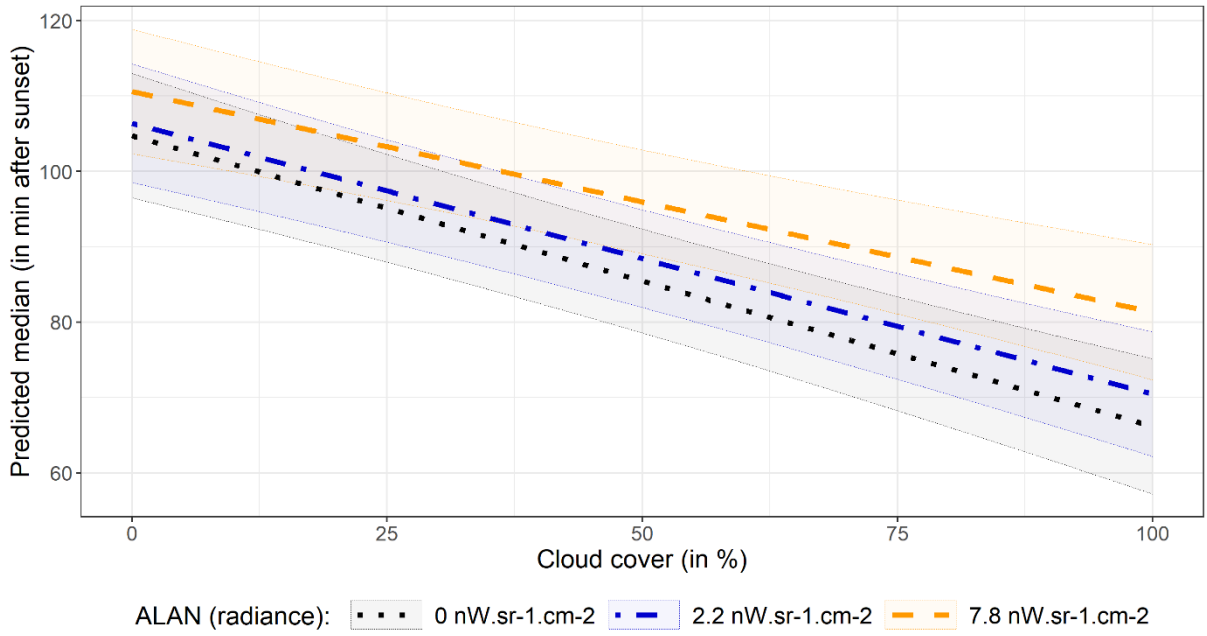

Figure O: Interaction between ALAN and moonlight: Predicted values and 95% confidence intervals of the timing of activity (i.e., the time of the median *E. serotinus* pass during the first half of the night) with all variables equal to zero (i.e., all variables equal to their mean, as they were previously scaled) apart from ALAN and moonlight. This graph represents the median time of activity according to ALAN (radiance back transformed in nW.sr^{-1}.cm^{-2}) for three values of moonlight.